HbV (liposome encapsulated hemoglobin) 膜への晶質，膠質浸透圧作用

三宅誠司[1)]，酒井宏水[2)]，高折益彦[3)]

1) 大阪府済生会野江病院検査科

2) Waseda Bioscience Research Institute in Singapore

3) 東宝塚さとう病院

和文要約 前回の研究で 蒸留水内包 liposome emulsion を一定濃度の食塩液と混合した時，とくに1:1容量混合でみられた食塩液中のNaイオン，Clイオンの予想以上の低下原因を明らかにするため以下の研究を行なった．研究1では前回使用したものと同質，同サイズのliposome粒子を0.4 g%アルブミンを含む0.625 g%の食塩液に浮遊させ，0，15，120分，24，168時間後にその食塩液中のNa，Clイオン濃度を測定した．その結果，実測したNa，Clイオン濃度はそれぞれ107.5 ± 0.7～108.4 ± 1.0 mEq/L，106,0 ± 0.7～106.5 ± 0.08 mEq/Lにあり，時間経過による変化は認められなかった．そしてliposome粒子内部の水分によってNa，Clイオン濃度が希釈されると推定した予測値にほぼ一致した．したがって前回の研究で認められたliposome emulsionを一定濃度の食塩液と混合した時にみられた予想以上のNaイオン，Clイオンの希釈は上記liposome粒子内部の水分の浮遊液への移動によると結論された．またその水分移動はliposome粒子と食塩液との混合後測定器が表示するまでの3.07 ± 0.03分以内に生じていたことが推定された．研究2では 0.625 g% 食塩液に上記 liposome 粒子を浮遊させた後にアルブミンを 4.0% になるように添加し，0，5，15，180 分に浮遊液中のNa，Cl濃度を測定した．その結果，Na，Clイオン濃度はそれぞれ149.4 ± 1.2～149.1 ± 1.2 mEq/L，139.9 ± 1.0～138.9 ± 1.2 mEq/Lであって，多少，時間経過とともに低下傾向，すなわちコロイド浸透圧によると思われるliposome粒子の内部の水分の移動傾向がみとめられたが統計学的には有意性を立証するに至らなかった．すなわち初期測定時から3時間測定時までで変化は認められなかった．そのため前回の研究での観察時間，3時間以内では少なくとも測定系に共存した4 g%アルブミンの膠質浸透圧はこのliposome粒子内部の水分の粒子外移動に関与していなかったことが確認された．

Microvascular Research 81 (2011) 169–176

Contents lists available at ScienceDirect

Microvascular Research

journal homepage: www.elsevier.com/locate/ymvre

Regular Article

Increased viscosity of hemoglobin-based oxygen carriers retards NO-binding when perfused through narrow gas-permeable tubes

Hiromi Sakai [a,b,*], Naoto Okuda [c], Shinji Takeoka [b,c], Eishun Tsuchida [a,†]

[a] Research Institute for Science and Engineering, Waseda University, Tokyo 169-8555, Japan
[b] Waseda Bioscience Research Institute in Singapore (WABIOS), Singapore 138667, Republic of Singapore
[c] Graduate School of Advanced Sciences and Engineering, Waseda University, Tokyo 162-8480, Japan

ARTICLE INFO

Article history:
Received 29 October 2010
Revised 7 December 2010
Accepted 9 December 2010
Available online 16 December 2010

Keywords:
Artificial oxygen carrier
Hemoglobin
Nitric oxide
Rheology
Gas reaction

ABSTRACT

Increased fluid viscosity of a solution of hemoglobin-based oxygen carriers (HBOCs) reduces vasoconstrictive effects because increased shear stress on the vascular wall enhances the production of vasorelaxation factors such as NO. Nevertheless, on a microcirculatory level, it remains unclear how viscosity affects the reaction of HBOCs and NO. In this study, different HBOCs were perfused through narrow gas-permeable tubes (25 μm inner diameter at 1 mm/s centerline velocity; hemoglobin concentration [Hb] = 5 g/dL). The reaction was examined microscopically based on the Hb visible-light absorption spectrum. When immersed in a NO atmosphere, the NO-binding of deoxygenated Hb solution (viscosity, 1.1 cP at 1000 s^{-1}) in the tube occurred about twice as rapidly as that of red blood cells (RBCs): 1.6 cP. Binding was reduced by PEGylation (PEG-Hb, 7.7 cP), by addition of a high molecular weight hydroxyethyl starch (HES) (2.8 cP), and by encapsulation to form Hb-vesicles (HbVs, 1.5 cP; particle size 279 nm). However, the reduction was not as great as that shown for RBCs. A mixture of HbVs and HES (6.2 cP) showed almost identical NO-binding to that of RBCs. Higher viscosity and particle size might reduce lateral diffusion when particles are flowing. The HbVs with HES showed the slowest NO-binding. Furthermore, Hb encapsulation and PEGylation, but not HES-addition, tended to retard CO-binding. Increased viscosity reportedly enhances production of endothelium NO. In addition, our results show that the increased viscosity also inhibits the reaction with NO. Each effect might mitigate vasoconstriction.

Introduction

Cell-free hemoglobin-based oxygen carriers (HBOCs) have been developed for use as alternative materials for use in transfusion. Some examples are intramolecular crosslinked hemoglobin (Hb), polymerized Hb, and polyethylene glycol conjugated Hb (Chang, 2004; Natanson et al., 2008). The major remaining hurdle before clinical approval of this earliest generation of cell-free HBOCs is vasoconstriction and resulting hypertension, which are presumably attributable to the high reactivity of Hb with endothelium-derived nitric oxide (NO) (Olson et al., 2004; Palmer et al., 1987; Yu et al., 2008, 2010). As a small molecule, Hb permeates the endothelial cell layer to spaces near smooth muscle, and inactivates NO there. However, cellular Hb-vesicles (HbVs) that encapsulate concentrated Hb solution in phospholipid vesicles (Sakai et al., 2008c; Tsuchida et al., 2009) induce neither vasoconstriction nor hypertension (Sakai et al., 2000a,b). The absence of vasoconstriction in the case of intravenous HbV injection might be related to the lowered NO-binding (Sakai et al., 2008a,b, 2010) and lowered permeability across the endothelial cell layer in the vascular wall.

That the vascular wall responds to the shear stress induced by blood flow is well documented. The wall dilates and releases endothelium-derived relaxation factors such as NO and prostacyclin (Chen et al., 1989; de Wit et al., 1997; Bertuglia, 2001). To minimize the vasoconstrictive action of HBOCs, increasing the fluid viscosity would be appropriate to increase the release of vasorelaxation factors (Intaglietta, 1999; Tsai et al., 2005; Salazar Vázquez et al., 2008). Reportedly, a viscous fluid of PEG-modified Hb developed by Sangart Inc. (San Diego, CA) shows no vasoconstriction (Vandegriff and Winslow, 2009; Manjula et al., 2003). However, it remains unclear how the increased fluid viscosity affects the binding profiles of endothelial-cell-derived NO and HBOCs. On the other hand, HBOCs show a high affinity to carbon monoxide (CO), and it is important to examine the reaction profile, because CO is endogenously produced by constitutive hemeoxygenase-2 in hepatocytes; it serves as a vasorelaxation factor in hepatic microcirculation. It is reported that small molecular Hb permeates across the fenestrated endothelium,

* Corresponding author. Waseda Bioscience Research Institute in Singapore, 11 Biopolis Way, #05-01/02 Helios, Singapore 138667. Fax: +65 6478 9416.
E-mail address: hirosakai@aoni.waseda.jp (H. Sakai).
† Emeritus Professor Eishun Tsuchida passed away during the preparation of this manuscript.

0026-2862/$ – see front matter © 2010 Elsevier Inc. All rights reserved.
doi:10.1016/j.mvr.2010.12.002

scavenges CO, and induces constriction of sinusoids and augments peripheral resistance (Goda et al., 1998).

Gas-permeable narrow tubes enable the measurement of the rates of O_2-release and CO-binding and NO-binding of HBOCs during their flow through the tubes at a practical Hb concentration (5–13 g/dL) (Sakai et al., 2003, 2010; Page et al., 1998). As described in this paper, we used gas-permeable narrow tubes made of perfluorinated polymer to study gas reaction profiles. We changed the viscosity of a Hb solution using PEGylation, by addition of water-soluble macromolecules, and by encapsulation in phospholipids, each of which is expected to be related to the mechanisms of vasoactive properties of HBOCs. The Hb concentration of PEG-Hb is difficult to increase through ultrafiltration because of its colloid osmotic pressure (Vandegriff et al., 1997). For that reason, we adjusted all HBOCs used for this study to 5 g/dL.

Materials and methods

Preparation of HbV, SFHb, Poly$_B$Hb, PEG-Hb, and human RBCs

With only slight modifications, HbVs were prepared using a method reported previously (Sakai et al., 1993, 2002; Sou et al., 2003). Human Hb solution was obtained through purification of outdated RBCs provided by the Japanese Red Cross Society (Tokyo, Japan) (Fig. 1). Then, Hb was stabilized by carbonylation (HbCO) and concentrated by ultrafiltration to 38 g/dL. Subsequently, pyridoxal 5′-phospate (PLP; Sigma Chemical Co., St. Louis, MO) was added to the HbCO solution as an allosteric effector at a molar ratio of PLP/Hb tetramer = 2.5. We use PLP instead of 2,3-diphosphoglyceric acid (2,3-DPG) because 2,3-DPG is chemically unstable. The Hb solution with PLP was then mixed with lipids and encapsulated in vesicles. The lipid bilayer comprised 1,2-dipalmitoyl-*sn*-glycero-3-phosphatidylcholine, cholesterol, 1,5-*O*-dihexadecyl-*N*-succinyl-L-glutamate (Nippon Fine Chemical Co. Ltd., Osaka, Japan), and 1,2-distearoyl-*sn*-glycerol-3-phosphatidylethanolamine-*N*-PEG$_{5000}$ (NOF Corp., Tokyo, Japan) at the molar composition of 5/5/1/0.033. The particle diameter was regulated using the extrusion method. The encapsulated HbCO was converted to HbO_2 by exposing the liquid membranes of HbVs to visible light under an O_2 atmosphere. Finally the Hb concentration of the suspension was adjusted to 5 g/dL or 10 g/dL. The particle size distribution was measured using a light-scattering method (Submicron Particle Size Analyzer, model N4 PLUS; Beckman Coulter Inc., Fullerton, CA).

Purified human Hb solution suspended in phosphate buffered saline (PBS) solution was prepared and mixed with PLP at molar ratios of PLP/Hb tetramer = 4 (Hb concentration = 5 or 10 g/dL).

To increase the viscosities of the HbV suspensions and Hb solutions, we used a high molecular weight hydroxyethyl starch, Hextend™, with Mw 670 kDa and 6 wt.% in a physiological Ringer lactate solution (HES solution) obtained from Hospira Inc. (Lake Forest, IL, USA). The volume ratios of HbV and Hb solutions ([Hb] = 10 g/dL) to HES were 50/50. Accordingly, the resulting Hb concentration became 5 g/dL.

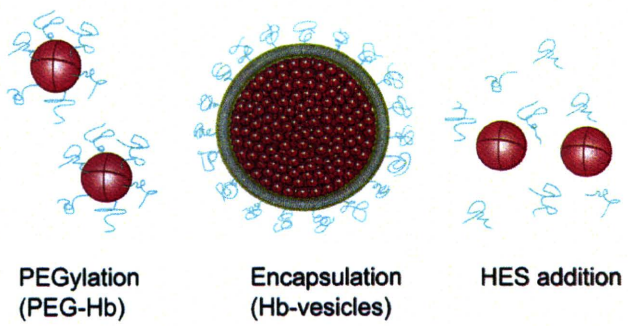

Fig. 1. Schematic representation of PEGylated Hb (PEG-Hb), encapsulated Hb (Hb-vesicles), and a simple mixture of HES and Hb to increase the viscosity of a Hb solution.

With some minor modifications, PEGylated human Hb (PEG-Hb) was prepared according to the method described in an earlier report (Vandegriff et al., 2003). The HbCO solution (5 g/dL, 50 mL, and 38.7 μM) in PBS was gently bubbled or flowed with nitrogen gas to remove O_2 in a sealed flask. Then, 15 times excess moles of 2-iminothiolane hydrochloride (IMT; Sigma Aldrich Corp.) were dissolved and stirred for 2.5 h in a dark anaerobic condition. Twenty times excess moles of α-[3-(3-maleimido-1-oxopropyl)amino]propyl-ω-methoxy PEG (Mal-PEG5000, Mr: 5552, Sunbright ME-050MA; NOF Corp.) were dissolved in the solution. The solution was kept anaerobic using a gentle N_2 and CO flow. After stirring for 3 h, the solution was diluted with 120 mL PBS and was ultrafiltrated using an appropriate system (cut off Mw. 50,000, polysulfone, 62 mm filter diameter; UHP-62 K; Advantec Co.). The dilution and ultrafiltration were repeated three times. Because of the high colloid osmotic pressure, ultrafiltration required high air pressure to permeate water. It was difficult to concentrate the Hb solution greater than 6 g/dL. Therefore, we selected Hb concentration of 5 g/dL for all the Hb-containing solutions. To convert HbCO to HbO_2, the PEG-HbCO solution was poured into a round flask and exposed to visible light of a halogen lamp. The flask was rotated and O_2 gas flowed into the flask. The photodissociated CO is emitted while O_2 binds to Hb.

For this study, we used fresh human blood specimens. The study was approved by Waseda University's Ethics Committee on Medical Research Involving Human Subjects (#2009-052), and performed according to the World Medical Association Declaration of Helsinki and Title 45, U.S. Code of Federal Regulations, Part 46, Protection of Human Subjects (Revised Nov. 13, 2001). A blood specimen was withdrawn after obtaining written informed consent from donors. It was mixed immediately with an anticoagulant; then RBCs were pelleted at 800×*g* for 30 min. They were resuspended and washed twice with PBS. The suspension was then filtrated through a leukocyte removal filter (Pall Corp., East Hills, NY). The RBC suspensions were prepared at a Hb concentration of 5 g/dL.

The P_{50} values and Hill numbers of HbVs, Hb solutions, and RBCs were obtained from the oxygen equilibrium curve measured using a Hemox Analyzer (TCS Scientific Corp., Philadelphia, PA) at 37 °C (Table 1). Steady-shear viscosity measurements were performed using a rheometer (Physica MCR 301; Anton Paar GmbH, Graz, Austria) at 25 °C.

Perfusion of Hb-containing fluids through narrow tubes

Narrow, gas-permeable tubes (25 μm inner diameter; 37.5 μm wall thickness; 150 mm length) were made of a fluorinated ethylene–propylene copolymer (Hirakawa Hewtech Corp., Ibaraki, Japan) as described in a previous report (Sakai et al., 2003, 2009a, 2010; Kubota et al., 1996) (Fig. 2). One end of the narrow tube was connected to a reservoir of the Hb-containing suspension. The narrow tube was immersed in a water bath (12 cm long × 3 cm width × 0.3 mm depth) made by two acrylic plates with a rubber supporting plate in between; it was placed horizontally on the stage of an inverted microscope (IX-71; Olympus Corp., Tokyo). The suspension in the reservoir was mixed gently and continuously using a magnetic stirrer (CC 301; AS One Corporation, Tokyo). It was then pressurized using a syringe connected to a syringe pump (FP-W-100; Toyo Sangyo Co. Ltd., Tokyo). The perfusion pressure was monitored using a digital pressure sensor (AP-C30; Keyence Co., Tokyo). The centerline flow velocity was analyzed using photodiodes and the cross-correlation technique (Velocity Tracker Mod-102 B; Vista Electronics Co., Ramona, CA) (Intaglietta et al., 1975). This method usually requires a significant change of contrasts because of the RBCs passing. However, stroma-free Hb, PEG-Hb, and HbVs are distributed homogeneously in the tube; no change of contrast is obtainable. Therefore, we added a small amount of RBCs (5 vol%) to enable centerline velocity measurements. This level of addition did not influence the reaction rate of the whole

Table 1
Physicochemical properties of HbVs, PEG-Hb, RBC, and Hb solutions, and mixtures of HES.

	HbVs	PEG-Hb	RBC	Hb	HbV + HES	Hb + HES
[Hb](g/dl)	5	5	5	5	5	5
Suspension medium	PBS	PBS	PBS	PBS	PBS + HES	PBS + HES
Hb/PLP, molar	1/2.5	–	–	1/4	–	1/4
$k'^{(CO)}_{ON}$ ($10^5\ M^{-1}\ s^{-1}$)	2.1[a]	3.8[b]	0.65[a]	2.1[a]	2.1[a]	2.1[a]
$k'^{(NO)}_{ON}$ ($10^7\ M^{-1}\ s^{-1}$)	0.61[a]	3.0[c]	0.012[a]	2.4[a]	0.61[a]	2.4[a]
P_{50} (Torr)	25–31	10.2	27	26	25–31	26
Size	279 nm	14.1 nm	8 μm	65 kDa	279 nm	65 kDa
Viscosity (cP)						
at $10^3\ s^{-1}$	1.49	7.71	1.56	1.12	6.20	2.96
at $10\ s^{-1}$	1.65	9.48	2.03	1.12	11.9	5.09
Flow pressure (kPa)	10.5–11.2	18.2–19.1	8.1–9.6	6.2–7.7	24.2–24.7	11.4–11.9

[a] (Sakai et al., 2008b);
[b] (Vandegriff et al., 2008);
[c] (Rohlfs et al., 1998).

solution: we confirmed that perfusion of saline with 5 vol% RBCs (without Hb or HbVs) provided a negligibly small light absorption spectrum. The centerline velocity was adjusted to 1 mm/s by changing the pressure applied to the reservoir. We selected the velocity of 1 mm/s in the tube and the gas concentrations (see below) to obtain the absorption changes in the 12-cm-long tube, as in our previous studies (Sakai et al., 2003, 2010).

The water bath was filled with saline containing 10 mM sodium hydrosulfite ($Na_2S_2O_4$; Wako Pure Chemical Industries Ltd., Tokyo) bubbled with low-concentration NO (NO, 4.7%; N_2, 95.3%) or CO (CO, 14.14%; N_2, 85.86%). Actually, $Na_2S_2O_4$ is effective to eliminate trace amounts of remaining oxygen that might affect the reactions of Hb and either NO or CO. The narrow tube wall is made of perfluorinated polymer and is permeable only by gas molecules: not by $Na_2S_2O_4$. The entire perfusion experiment was performed at 25 °C. In our experiment, the inner volume of the narrow tube was 5.9×10^{-5} cm^3, which is much smaller (1/180,000) than the volume of the exterior water bath (11 cm^3). We assumed that NO or CO is abundant in the exterior area and that it was provided continuously into the tube in the binding experiment.

Equipment to monitor gas reactions in narrow tubes

The apparatus consisted of an inverted microscope with an objective lens of ×40 magnification (ULWD CDPlan 40PL; Olympus Corp.), a spectrophotometer (Photonic multi- channel analyzer Model PMA-11; Hamamatsu Photonics KK, Hamamatsu, Japan) connected through a C-mount, a thin optical guide, and a computer (FMV Biblio MG50R; Fujitsu Co. Ltd., Tokyo). The microscope's light source (a halogen lamp) intensity was controlled using a current stabilizer (TH4-100; Olympus Corp.). The scanned wavelength was 194–956 nm with a gate time of 100 ms/scan; data were obtained every 0.2 nm. One spectrum from a 25-μm-diameter spot over the centerline of the narrow tube was recorded and 100 scans were accumulated in 10 s. A measuring spot on the narrow tube within the visual field of the microscope was fixed on a monitor (PVM-14L2; Sony Corp., Tokyo) through a CCD camera (Model CS 230B; Olympus Corp.) by sliding the microscope stage.

Measurement of NO-binding rate of deoxygenated Hb-containing solutions

To measure the NO-binding rate, the tube was immersed in a saline solution containing 10 mM $Na_2S_2O_4$, which had been previously bubbled with a gas of 4.7% NO/N_2 balance (Takachiho Chemical Industrial Co. Ltd., Tokyo). The resultant NO concentration outside of the tube was approximately 88 μM. Spectroscopic measurements were performed at traveling distances of 10–90 mm. Three measurements were performed after a steady flow was attained. In the spectra of the 100%-deoxygenated and 100%-nitrosyl Hb-containing samples, two isosbestic points (449 and 592 nm) were connected by a straight line as the baseline (Sakai et al., 2010; Vandegriff et al., 1997). Absorbance data at 555 nm (A_{555}, λ_{max} of deoxyHb) and 575 nm (A_{575}, λ_{max} of HbNO) from the baseline were obtained to produce a calibration line showing the relation between the NO saturation (in %) and the ratio of the two absorbances ($R = A_{555}/A_{575}$) (Fig. 3). The NO saturation values of each sample were averaged. They are shown versus the traveling distance ($n = 3$, mean ± standard deviation).

Measurement of CO-binding rate of deoxygenated Hb-containing solutions

The method used to measure the CO-binding rate is fundamentally identical to that of the NO-binding rate. A gas of 14.14% CO/N_2 balance (Takachiho Chemical Industrial Co. Ltd.) was used to attain the CO

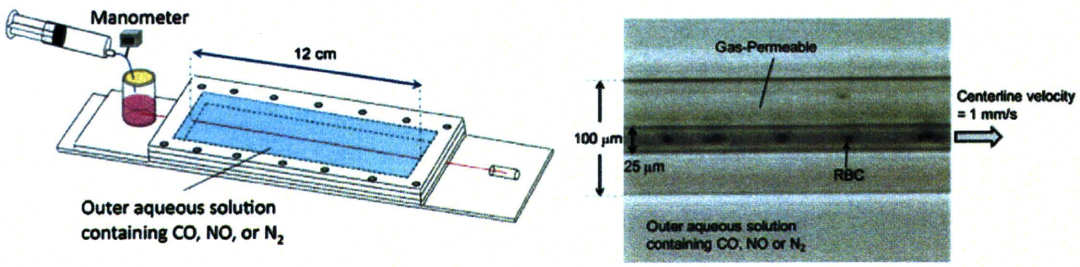

Fig. 2. (left) Schematic view of the experimental setup of a gas-permeable artificial narrow tube (red line) immersed in a water bath (light blue) produced by the gap separating two transparent acrylic plates with a rubber supporting plate. One end of the narrow tube was connected to a reservoir (pink) of the Hb-containing suspension. The reservoir is pressurized using N_2 gas for perfusion of a fluid through the tube. (right) Microscopic view of a gas-permeable artificial narrow tube. The tube, made of perfluorinated polymer, is gas-permeable. The tube is immersed in water equilibrated with low-concentration CO, or NO gases.

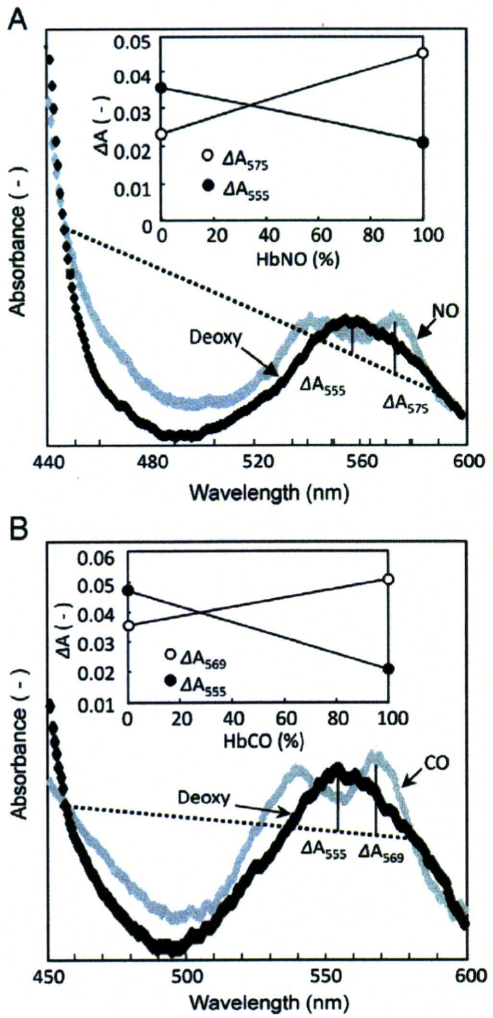

Fig. 3. Calculation of reaction levels (A) HbNO and (B) HbCO from the absorption changes. For the determination of HbNO level, for example, two isosbestic points of the spectra of deoxygenated and nitrosyl HbVs (at 449 and 592 nm) were connected by a straight line (baseline). Based on absorbances at 555 (ΔA_{555}, λ_{max} of deoxyHb) and 576 (ΔA_{575}, λ_{max} of HbNO) nm from the baseline, linear relations between the level of HbNO (%) and ΔA_{555} and ΔA_{575} are obtained individually as depicted in the inset. The ratio of the two absorbances ($R = A_{555}/A_{575}$) was used to obtain the level of HbNO. The levels of HbCO (B) were calculated similarly.

concentration: approximately 135 μM. Two isosbestic points (454 and 578 nm) of HbCO and deoxyHb were obtained (Sakai et al., 2010). The absorbance data obtained at 555 nm (A_{555}, λ_{max} of deoxyHb) and 575 nm (A_{569}, λ_{max} of HbCO) from the baseline were used to obtain the calibration curve of CO saturation (in %) versus $R = A_{555}/A_{569}$.

Results

NO-binding profile

All Hb-containing solutions showed a change of absorption spectroscopy in the Q band region (Fig. 4). Before NO-binding, they showed a single peak at 555 nm attributable to deoxyHb (top red lines). The absorption spectrum changes gradually with the traveling distance. Two new peaks tended to appear at 545 nm and 575 nm (blue and green lines), indicating the conversion of deoxyHb to HbNO (bottom red lines, 100% HbNO). Fig. 5 shows the change of the level of HbNO saturation of all the Hb-containing samples. The NO-binding profile of the stroma-free Hb solution is the fastest; that of RBCs is the slowest. The HbNO level of Hb solution was 94 ± 6% at 5 cm traveling distance, whereas RBC showed only 39 ± 1% at 5 cm traveling distance. Each of the Hb encapsulation (HbV, 71 ± 10%), PEGylation (PEG-Hb, 73 ± 2%), and HES-addition (Hb + HES, 66 ± 7%) showed retardation of NO-binding to some degree. However, they were much faster than RBCs. The HbVs suspended in HES (HbV + HES, 37 ± 3%) showed similar NO-binding profiles to those of RBCs.

CO-binding profile

Figure 6 shows that deoxyHb with a single peak at 555 nm (top red lines) in the Q band changes gradually. Two new peaks tended to appear at 540 nm and 569 nm (blue and green lines), reflecting the conversion of deoxyHb to HbCO (bottom red lines, 100% HbCO). Figure 7 shows that the HbCO conversion rates of Hb and RBCs differed considerably. The Hb solution showed a much higher CO-binding rate than that of RBCs (90 ± 3% for Hb, 53 ± 2% for RBC at 5 cm traveling distance). The Hb encapsulation (HbV, 76 ± 6%) and PEGylation (73 ± 4%) showed retardation of CO-binding to some degree, but they are still faster than those of RBC. Addition of HES to both the Hb solution and HbVs did not seem to change the CO-binding rate.

Discussion

Our primary finding is that the NO-binding reaction of the Hb solution is retarded by encapsulation (HbVs), PEGylation (PEG-Hb), and simple HES-addition to the Hb solution when perfused through an artificial narrow plastic tube at Hb concentration of 5 g/dL. However, they showed much faster binding than RBCs did. The combination of HbVs and HES considerably retarded the NO-binding rate and showed a similar rate to that of RBCs. However, slight retardation of CO-binding was shown by encapsulation and PEGylation; the addition of HES showed no further retardation.

Conditions of hemolysis and studies related to the development of HBOCs have shown that entrapment of endothelium-derived NO induces vasoconstriction, hypertension, reduced blood flow, and vascular damage (Minneci et al., 2005; Natanson et al., 2008; Olson et al., 2004; Hess et al., 1993; Nakai et al., 1996, 1998; Rochon et al., 2004; Sloan et al., 1999). Physiological doses of CO are a vasorelaxation factor, especially in the hepatic microcirculation. Its entrapment by cell-free Hb solutions induces constriction of sinusoidal capillaries (Goda et al., 1998). These side effects caused by the presence of molecular Hb in plasma suggest that the cellular structure of RBCs plays a role in ensuring the bioavailability of NO and CO.

The suspension of HbVs has no colloid osmotic pressure. It is a particle dispersion that can be concentrated easily to [Hb] = 10 g/dL. In an earlier study, we measured the NO-binding rates of HbVs, stroma-free Hb, polymerized Hb, and RBC at 10 g/dL using the same experimental setup (Sakai et al., 2010). However, we were unable to measure PEG-Hb because it has a considerably high colloid osmotic pressure that hinders ultrafiltration. The maximum Hb concentration was as low as 6 g/dL (Sakai et al., 2000b; Vandegriff et al., 1997). One very promising material developed by Sangart Inc., PEG-Hb, is now in the final stages of clinical trials (Vandegriff and Winslow, 2009). Therefore, it is quite interesting to compare HbVs and PEG-Hb under identical conditions. In this study, we measured the NO-binding rates of these materials at [Hb] = 5 g/dL. Results show that PEG-Hb and HbVs exhibited similar NO-binding rates; they are slower than the stroma-free Hb solutions. This low rate is plausible because both PEG-Hb and HbVs reportedly show no vasoconstriction (Sakai et al., 2000a; Vandegriff et al., 2003). The retardation of NO-binding is induced by the lowered lateral diffusion and inefficient lateral fluid mixing effect when they flow through the narrow tube, according to our previous report (Sakai et al., 2010). The NO molecules that diffuse through the tube wall and enter the lumen would immediately react with Hb-

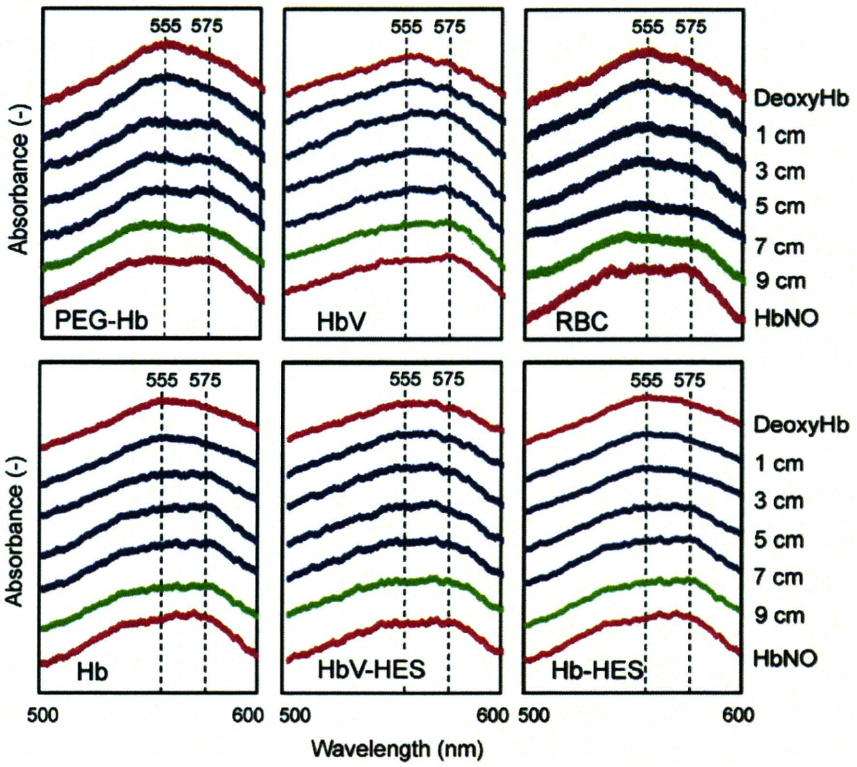

Fig. 4. Spectroscopic changes in *Q* bands of the Hb-containing fluids by NO-binding during perfusion through the narrow tube at traveling distances of 1–9 cm. Red plot lines show the absorption spectra of 0% and 100% reactions. Green lines show spectra at 9 cm traveling distance. Two characteristic new peaks attributed to HbNO ($\lambda_{max} = 545$ and 575 nm) increased with the traveling distance; deoxyHb (555 nm) decreased.

containing solutions at the interface. Therefore, fast mixing would be effective to create more NO-binding sites. Both viscosity and particle size influence such lateral diffusion. Actually, PEG-Hb shows a higher viscosity (7.7 cP at $10^3\ s^{-1}$) than that of the Hb solution. It is particularly interesting that the simple addition of HES to Hb increased the viscosity from 1.12 to 2.96 cP, and that it retarded NO-binding. Having a large diameter (279 nm), HbVs contributed to the retardation of the lateral diffusion. However, all these measures – encapsulation, PEGylation, and polymer-addition to Hb – were insufficient to retard the NO-binding to the level of RBCs.

It is quite noteworthy that all the gas reactions of RBCs are much slower than those of Hb solution and HBOCs. In our previous report of gas reactions in a diluted Hb-containing solution using the stopped flow rapid scan spectrophotometry and computer simulation, we clarified that the retardation of NO- and CO-bindings are due to the intracellular diffusion barrier created by the intracellular concentrated Hb solution (Sakai et al., 2008a). We suggested that the cell membrane does not seem to have a barrier function to gas diffusion and that the unstirred layer surrounding the cell surface would not be a major factor because of the rapid mixing at stopped flow method. In the present study we could measure the gas reactions at a practical Hb concentration in a flowing condition, which is more relevant to a physiological condition. RBCs tend to flow centerline and plasma layer (RBC-free layer) is created (Sakai et al., 2009a), which becomes a diffusion barrier for gas molecules (Vaughn et al., 1998; Butler et al., 1998; Tsoukias, 2008). This is in contrast to the molecules and particles of Hb, PEG-Hb, and HbV which are much smaller than those of RBCs. They are distributed homogeneously in the plasma phase in the tube. It is particularly interesting that addition of a high-molecular-weight HES to HbVs showed a considerably retarded NO-binding rate to the level of RBCs. The viscosity of the HbV suspension at [Hb] = 5 g/dL was 1.6 cP, which is nearly identical to that of RBC. Addition of HES to HbVs increased the viscosity to 6.2 cP because of the flocculation of HbVs through depletion interaction (Sakai et al., 2007, 2009b). The higher viscosity and larger size of flocculated HbVs are expected to contribute to the reduced lateral diffusion. Even though the flocculated HbVs dissociate at a higher shear rate, it is speculated that they would create a plasma layer of lowered HbV concentration just nearby the inner wall that might become a gas diffusion barrier, and retard the gas reactions significantly.

Even though the NO-binding rates differ considerably among samples, the CO-binding rates did not differ greatly because of the fundamentally lower CO-binding rate constants of the Hb-containing samples in comparison with the NO-binding rate constants, as shown

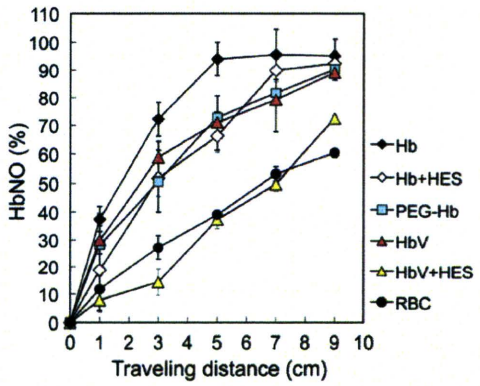

Fig. 5. Change of the level of NO-binding reactions of the Hb-containing fluids, Hb solution (black rhombi), PEG-Hb (blue squares), HbV (pink triangles), Hb + HES (white rhombi), HbV + HES (yellow triangles), and RBC (black circles) with traveling distance.

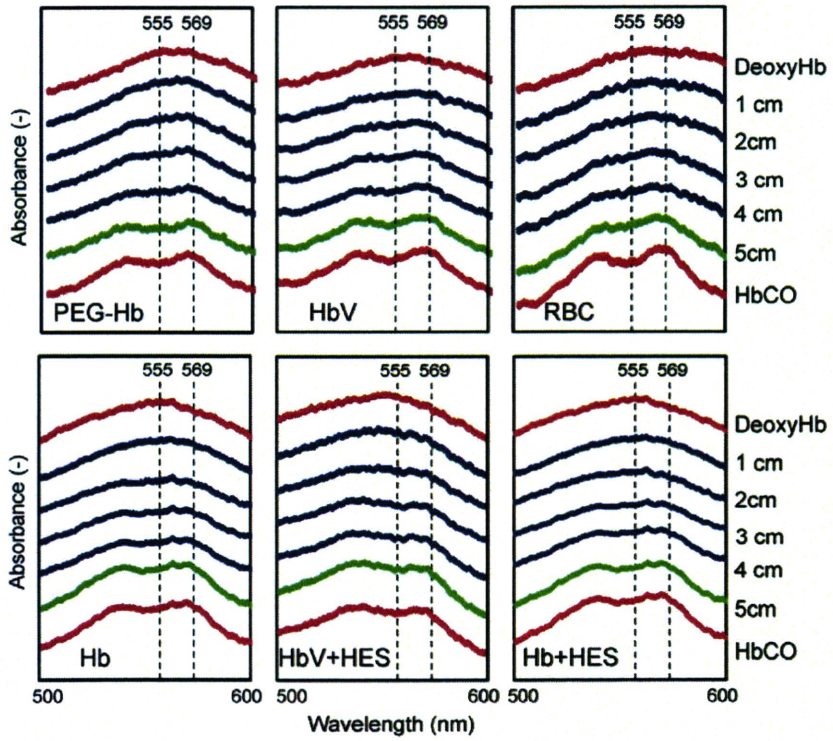

Fig. 6. Spectroscopic changes in Q bands of the Hb-containing fluids with CO-binding perfused through the narrow tube. Two new characteristic peaks attributed to HbCO (λ_{max} = 540 and 569 nm) increased with the traveling distance; deoxyHb (555 nm) decreased.

in Table 1. The NO gas molecules diffused through the tube inner wall bind rapidly to Hb. In contrast, CO gas has more time to diffuse in the inner fluid to bind to Hb. That CO-binding is retarded slightly by encapsulation and PEGylation, but we were unable to produce clear retardation to the level of RBCs merely by the addition of HES to HbV.

One limitation of our experimental setup for evaluating NO reactions is that we cannot measure the reaction of NO and HbO_2 to form metHb and nitrate, even though this reaction is predominant in *in vivo* blood circulation. In our system in Figure 2, the narrow tube is immersed in a solution bubbled with NO/N_2 mixed gas (oxygen tension is zero). Perfusion of HbO_2 in the tube causes not only metHb and nitrate formation but also deoxygenation and NO-binding to deoxygenated Hb. Accordingly we did not have the experiment of the reaction of NO and HbO_2. However, we speculate that such reaction would be more influenced by the increased viscosity, because the reaction rate constant of NO and HbO_2 ($k_{ox}^{(NO)} = 8.7 \times 10^7\ M^{-1}\ s^{-1}$) is essentially larger than that of NO-binding ($k_{on}^{(NO)} = 2.4 \times 10^7\ M^{-1}\ s^{-1}$) and CO-binding ($k_{on}^{(CO)} = 2.1 \times 10^5\ M^{-1}\ s^{-1}$) (Sakai et al., 2008b) in the order, $k_{ox}^{(NO)} > k_{on}^{(NO)} > k_{on}^{(CO)}$, and the gas reaction would be completed at the closer place to the inner wall.

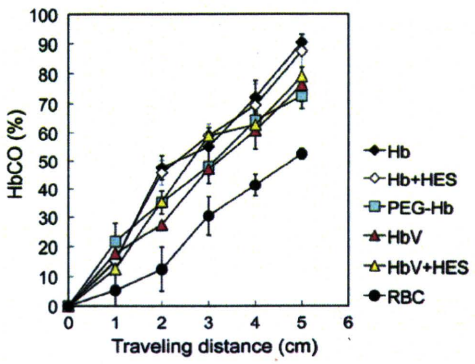

Fig. 7. Change of the level of CO-binding reactions of the Hb-containing fluids, Hb solution (black rhombi), PEG-Hb (blue squares), HbV (pink triangles), Hb + HES (white rhombi), HbV + HES (yellow triangles), and RBC (black circles) with traveling distance.

One remaining question is whether the retarded NO-binding and CO-binding rates found in this study are sufficient to explain the absence or presence of vasoconstriction. We infer the presence of a threshold particle diameter not only in terms of diffusiveness in the plasma phase, as discussed herein, but also in terms of penetration across the perforated endothelial cell layer to approach a space (such as the space of Disse near the sinusoidal endothelial layer in a hepatic microcirculation, or the space between the endothelium and the smooth muscle). At that space, CO or NO is produced as a vasorelaxation factor to bind to soluble guanylate cyclase, which catalyzes the conversion of guanosine triphosphate to cyclic guanosine monophosphate (Sakai et al., 2000a; Nakai et al., 1998; Goda et al., 1998; Matheson et al., 2002). At the very least, both HbVs and PEG-Hb are unable to permeate across the endothelial layers in the vascular wall. As summarized by Olson et al. (2004) both the retardation of the NO reaction (reduced NO affinity) and the larger particle diameter are inferred to be keys to suppression of vasoconstriction and hypertension induced by HBOCs because the simple combination of Hb solution and HES would not prevent vasoconstriction even if the mixed fluid were highly viscous.

Conclusion

In summary, results of this study clarified that increased viscosity or increased size can reduce the gas reaction rates for NO-binding, probably because of the lowered lateral diffusivity in the tube. That can partly explain the mechanism of vasoconstriction. Several biological mechanisms of vasoconstriction other than gas reactions are reported, such as induction of hypersensitivity of adrenergic receptors and plasma enthothelin-1 increase (Gulati et al., 1999). Reportedly, increased viscosity of HBOCs is effective to increase the

shear stress on the vascular wall and enhance production of vasorelaxation factor. In our study, we additionally uncovered advantages of increased viscosity, and retardation of HBOCs reaction with NO as vasorelaxation factors. This finding will be important to encourage reconsideration of the design of the optimal HBOC chemical structure.

Conflict of interest

Of the authors, HS, ST, and ET are the inventors of patents related to the production and utilization of Hb-vesicles.

Acknowledgments

We thank Dr. Nobuji Maeda and Dr. Yoji Suzuki (Ehime University) for the experimental setup. This work was supported in part by Health and Labour Science Research Grants (Health Science Research Including Drug Innovation), Ministry of Health, Labour and Welfare, Japan (H.S.), Grants-in-Aid for Scientific Research from the Japan Society for the Promotion of Science (B19300164; B22300161) (H.S.), and a Supporting Project to Form Strategic Research Platforms for Private Universities: Matching Fund Subsidy from Ministry of Education, Culture, Sports, Science and Technology.

References

Bertuglia, S., 2001. Increased viscosity is protective for arteriolar endothelium and microvascular perfusion during severe hemodilution in hamster cheek pouch. Microvasc. Res. 61, 56–63.

Butler, A.R., Megson, I.L., Wright, P.G., 1998. *Diffusion of nitric oxide and scavenging by blood in the vasculature.*

Chang, T.M., 2004. Hemoglobin-based red blood cell substitutes. Artif. Organs 28, 789–794.

Chen, R.Y., Carlin, R.D., Simchon, S., Jan, K.M., Chien, S., 1989. Effects of dextran-induced hyperviscosity on regional blood flow and hemodynamics in dogs. Am. J. Physiol. Heart Circ. Physiol. 256, H898–H905.

de Wit, C., Schäfer, C., von Bismarck, P., Bolz, S.S., Pohl, U., 1997. Elevation of plasma viscosity induces sustained NO-mediated dilation in the hamster cremaster microcirculation in vivo. Pflugers Arch. 434, 354–361.

Goda, N., Suzuki, K., Naito, M., Takeoka, S., Tsuchida, E., Ishimura, Y., Tamatani, T., Suematsu, M., 1998. Distribution of heme oxygenase isoforms in rat liver. Topographic basis for carbon monoxide-mediated microvascular relaxation. J. Clin. Invest. 101, 604–612.

Gulati, A., Barve, A., Sen, A.P., 1999. Pharmacology of hemoglobin therapeutics. J. Lab. Clin. Med. 133, 112–119.

Hess, J.R., MacDonald, V.W., Brinkley, W.W., 1993. Systemic and pulmonary hypertension after resuscitation with cell-free hemoglobin. J. Appl. Physiol. 74, 1769–1778.

Intaglietta, M., 1999. Microcirculatory basis for the design of artificial blood. Microcirculation 6, 247–258.

Intaglietta, M., Silverman, N.R., Tompkins, W.R., 1975. Capillary flow velocity measurements in vivo and in situ by television methods. Microvasc. Res. 10, 165–179.

Kubota, K., Tamura, J., Shirakura, T., Kimura, M., Yamanaka, K., Isozaki, T., Nisho, I., 1996. The behaviour of red cells in narrow tubes in vitro as a model of the microcirculation. Br. J. Haematol. 94, 266–272.

Manjula, B.N., Tsai, A., Upadhya, R., Perumalsamy, K., Smith, P.K., Malavalli, A., Vandegriff, K., Winslow, R.M., Intaglietta, M., Prabhakaran, M., Friedman, J.M., Acharya, A.S., 2003. Site-specific PEGylation of hemoglobin at Cys-93β: correlation between the colligative properties of the PEGylated protein and the length of the conjugated PEG chain. Bioconjug. Chem. 14, 464–472.

Matheson, B., Kwansa, H.E., Bucci, E., Rebel, A., Koehler, R.C., 2002. Vascular response to infusions of a nonextravasating hemoglobin polymer. J. Appl. Physiol. 93, 1479–1486.

Minneci, P.C., Deans, K.J., Zhi, H., Yuen, P.S., Star, R.A., Banks, S.M., Schechter, A.N., Natanson, C., Gladwin, M.T., Solomon, S.B., 2005. Hemolysis-associated endothelial dysfunction mediated by accelerated NO inactivation by decompartmentalized oxyhemoglobin. J. Clin. Invest. 115, 3409–3417.

Nakai, K., Ohta, T., Sakuma, I., Akama, K., Kobayashi, Y., Tokuyama, S., Kitabatake, A., Nakazato, Y., Takahashi, T.A., Sekiguchi, S., 1996. Inhibition of endothelium-dependent relaxation by hemoglobin in rabbit aortic strips: comparison between acellular hemoglobin derivatives and cellular hemoglobins. J. Cardiovasc. Pharmacol. 28, 115–123.

Nakai, K., Sakuma, I., Ohta, T., Ando, J., Kitabatake, A., Nakazato, Y., Takahashi, T.A., 1998. Permeability characteristics of hemoglobin derivatives across cultured endothelial cell monolayers. J. Lab. Clin. Med. 132, 313–319.

Natanson, C., Kern, S.J., Lurie, P., Banks, S.M., Wolfe, S.M., 2008. Cell-free hemoglobin-based blood substitutes and risk of myocardial infarction and death: a meta-analysis. JAMA 299, 2304–2312.

Olson, J.S., Foley, E.W., Rogge, C., Tsai, A.L., Doyle, M.P., Lemon, D.D., 2004. No scavenging and the hypertensive effect of hemoglobin-based blood substitutes. Free Radic. Biol. Med. 36, 685–697.

Page, T.C., Light, W.R., McKay, C.B., Hellums, J.D., 1998. Oxygen transport by erythrocyte/hemoglobin solution mixtures in an in vitro capillary as a model of hemoglobin-based oxygen carrier performance. Microvasc. Res. 55, 54–66.

Palmer, R.M.J., Ferrige, A.G., Moncada, S., 1987. Nitric-oxide release accounts for the biological- activity of endothelium-derived relaxing factor. Nature 327, 524–526.

Rochon, G., Caron, A., Toussaint-Hacquard, M., Alayash, A.I., Gentils, M., Labrude, P., Stoltz, J.F., Menu, P., 2004. Hemodilution with stroma-free hemoglobin at physiologically maintained viscosity delays the onset of vasoconstriction. Hypertension 43, 1110–1115.

Rohlfs, R.J., Bruner, E., Chiu, A., Gonzales, A., Gonzales, M.L., Magde, D., Magde Jr., M.D., Vandegriff, K.D., Winslow, R.M., 1998. Arterial blood pressure responses to cell-free hemoglobin solutions and the reaction with nitric oxide. J. Biol. Chem. 273, 12128–12134.

Sakai, H., Takeoka, S., Yokohama, H., Seino, Y., Nishide, H., Tsuchida, E., 1993. Purification of concentrated hemoglobin using organic solvent and heat treatment. Protein Expr. Purif. 4, 563–569.

Sakai, H., Hara, H., Yuasa, M., Tsai, A.G., Takeoka, S., Tsuchida, E.M., Intaglietta, M., 2000a. Molecular dimensions of Hb-based O_2 carriers determine constriction of resistance arteries and hypertension. Am. J. Physiol. Heart Circ. Physiol. 279, H908–H915.

Sakai, H., Yuasa, M., Onuma, H., Takeoka, S., Tsuchida, E., 2000b. Synthesis and physicochemical characterization of a series of hemoglobin-based oxygen carriers: objective comparison between cellular and acellular types. Bioconjug. Chem. 11, 56–64.

Sakai, H., Masada, Y., Takeoka, S., Tsuchida, E., 2002. Characteristics of bovine hemoglobin as a potential source of hemoglobin-vesicles for an artificial oxygen carrier. J. Biochem. (Tokyo) 131, 611–617.

Sakai, H., Suzuki, Y., Kinoshita, M., Takeoka, S., Maeda, N., Tsuchida, E., 2003. O_2 release from Hb vesicles evaluated using an artificial, narrow O_2-permeable tube: comparison with RBCs and acellular Hbs. Am. J. Physiol. Heart Circ. Physiol. 285, H2543–H2551.

Sakai, H., Sato, A., Takeoka, S., Tsuchida, E., 2007. Rheological properties of hemoglobin vesicles (artificial oxygen carriers) suspended in a series of plasma-substitute solutions. Langmuir 23, 8121–8128.

Sakai, H., Sato, A., Masuda, K., Takeoka, S., Tsuchida, E., 2008a. Encapsulation of concentrated hemoglobin solution in phospholipid vesicles retards the reaction with NO, but not CO, by intracellular diffusion barrier. J. Biol. Chem. 283, 1508–1517.

Sakai, H., Sato, A., Sobolewski, P., Takeoka, S., Frangos, J.A., Kobayashi, K., Intaglietta, M., Tsuchida, E., 2008b. NO and CO binding profiles of hemoglobin vesicles as artificial oxygen carriers. Biochim. Biophys. Acta 1784, 1441–1447.

Sakai, H., Sou, K., Horinouchi, H., Kobayashi, K., Tsuchida, E., 2008c. Haemoglobin-vesicles as artificial oxygen carriers: present situation and future visions. J. Intern. Med. 263, 4–15.

Sakai, H., Sato, A., Okuda, N., Takeoka, S., Maeda, N., Tsuchida, E., 2009a. Peculiar flow patterns of RBCs suspended in viscous fluids and perfused through narrow tubes (25 μm). Am. J. Physiol. Heart Circ. Physiol. 297, H583–H589.

Sakai, H., Sato, A., Takeoka, S., Tsuchida, E., 2009b. Mechanism of flocculate formation of highly concentrated phospholipid vesicles suspended in a series of water-soluble biopolymers. Biomacromolecules 10, 2344–2350.

Sakai, H., Okuda, N., Sato, A., Yamaue, T., Takeoka, S., Tsuchida, E., 2010. Hemoglobin encapsulation in vesicles retards NO and CO binding and O_2 release when perfused through narrow gas-permeable tubes. Am. J. Physiol. Heart Circ. Physiol. 298, H956–H965.

Salazar Vázquez, B.Y., Wettstein, R., Cabrales, P., Tsai, A.G., Intaglietta, M., 2008. Microvascular experimental evidence on the relative significance of restoring oxygen carrying capacity vs. blood viscosity in shock resuscitation. Biochim. Biophys. Acta 1784, 1421–1427.

Sloan, E.P., Koenigsberg, M., Gens, D., Cipolle, M., Runge, J., Mallory, M.N., Rodman Jr., G., 1999. Diaspirin cross-linked hemoglobin (DCLHb) in the treatment of severe traumatic hemorrhagic shock: a randomized controlled efficacy trial. JAMA 282, 1857–1864.

Sou, K., Naito, Y., Endo, T., Takeoka, S., Tsuchida, E., 2003. Effective encapsulation of proteins into size-controlled phospholipid vesicles using freeze-thawing and extrusion. Biotechnol. Prog. 19, 1547–1552.

Tsai, A.G., Acero, C., Nance, P.R., Cabrales, P., Frangos, J.A., Buerk, D.G., Intaglietta, M., 2005. Elevated plasma viscosity in extreme hemodilution increases perivascular nitric oxide concentration and microvascular perfusion. Am. J. Physiol. Heart Circ. Physiol. 288, H1730–H1739.

Tsoukias, N.M., 2008. Nitric oxide bioavailability in the microcirculation: insights from mathematical models. Microcirculation 15, 813–834.

Tsuchida, E., Sou, K., Nakagawa, A., Sakai, H., Komatsu, T., Kobayashi, K., 2009. Artificial oxygen carriers, hemoglobin vesicles and albumin-hemes, based on bioconjugate chemistry. Bioconjug. Chem. 20, 1419–1440.

Vandegriff, K.D., Winslow, R.M., 2009. Hemospan: design principles for a new class of oxygen therapeutic. Artif. Organs 33, 133–138.

Vandegriff, K.D., McCarthy, M., Rohlfs, R.J., Winslow, R.M., 1997. Colloid osmotic properties of modified hemoglobins: chemically cross-linked versus polyethylene glycol surface-conjugated. Biophys. Chem. 69, 23–30.

Vandegriff, K.D., Malavalli, A., Wooldridge, J., Lohman, J., Winslow, R.M., 2003. MP4, a new nonvasoactive PEG-Hb conjugate. Transfusion 43, 509–516.

Vandegriff, K.D., Young, M.A., Lohman, J., Bellelli, A., Samaja, M., Malavalli, A., Winslow, R.M., 2008. CO-MP4, a polyethylene glycol-conjugated haemoglobin derivative and carbon monoxide carrier that reduces myocardial infarct size in rats. Br. J. Pharmacol. 154, 1649–1661.

Vaughn, M.W., Kuo, L., Liao, J.C., 1998. Estimation of nitric oxide production and reaction rates in tissue by use of mathematical model. Am. J. Physiol. Heart Circ. Physiol. 274, H2163–H2176.

Yu, B., Raher, M.J., Volpato, G.P., Bloch, K.D., Ichinose, F., Zapol, W.M., 2008. Inhaled nitric oxide enables artificial blood transfusion without hypertension. Circulation 117, 1982–1990.

Yu, B., Shahid, M., Egorina, E.M., Sovershaev, M.A., Raher, M.J., Lei, C., Wu, M.X., Bloch, K.D., Zapol, W.M., 2010. Endothelial dysfunction enhances vasoconstriction due to scavenging of nitric oxide by a hemoglobin-based oxygen carrier. Anesthesiology 112, 586–594.

Heart Vessels (2010) 25:417–425
DOI 10.1007/s00380-009-1222-6

ORIGINAL ARTICLE

Tadashi Yamagishi · Motoaki Bessho · Shigeki Yanagida
Kenya Nishizawa · Masatoshi Kusuhara
Fumitaka Ohsuzu · Seiichi Tamai

Severe, short-term food restriction improves cardiac function following ischemia/reperfusion in perfused rat hearts

Received: March 23, 2009 / Accepted: November 19, 2009

Abstract The purpose of this study was to clarify the characteristics of improved ischemic tolerance induced by severe, short-term food restriction in isolated, perfused rat hearts. Male Wistar (8 week-old) rats were given a food intake equivalent to a 70% reduction on the food intake of ad-libitum fed rats for 11 days (FR group and AL group, respectively). After this period, hearts were isolated and perfused in the Langendorff mode, and subjected to 20 min of global ischemia followed by 30 min of reperfusion. Although the coronary flow rate in the FR group (63.0 ± 3.1 ml/min/g dry weight) was higher than that in the AL group (47.1 ± 1.3 ml/min/g dry weight) during preischemic perfusion, the lactate release into the coronary effluent and absolute values of +dP/dt and –dP/dt in the FR group (2422 ± 161 and –1282 ± 51) were inversely lower than in the AL group (2971 ± 156 and –1538 ± 74, respectively). An increase in ischemic contracture was suppressed in the FR group. Following reperfusion, cardiac function, high-energy phosphate content, and intracellular pH, as measured by ^{31}P-nuclear magnetic resonance spectroscopy, had recovered to a much greater degree in the FR group than in the AL group. The serum T_3 level was significantly lower in the FR group (2.7 ± 0.1 pg/ml) than in the AL group (3.6 ± 0.1 pg/ml), and the levels of triglycerides, free fatty acids, insulin, and glucose were also significantly lower in the FR group than in the AL group. The protein expressions of myocyte enhancer factor 2A, Na^+,K^+-ATPase, and phospholamban in the cardiac tissue were higher in the FR group than in the AL group. These results suggested that severe, short-term food restriction improves ischemic tolerance in rat hearts via altered expression of functional proteins induced by low serum T3 levels, decreased coronary conductance, and change in metabolic flux.

T. Yamagishi (✉) · S. Tamai
Department of Laboratory Medicine, National Defense Medical College, 3-2 Namiki, Tokorozawa, Saitama 359-8513, Japan
Tel. +81-42-995-1597; Fax +81-42-996-5200
e-mail: grd1418@kmh.gr.jp

M. Bessho · S. Yanagida · K. Nishizawa · M. Kusuhara · F. Ohsuzu
First Department of Internal Medicine, National Defense Medical College, Saitama, Japan

Key words Caloric restriction · Glycolysis · Lactate · Phosphorus · Reperfusion injury

Introduction

Calorie restriction (CR) has been shown to extend life span, decrease age-related physiological changes, and delay cancer progress in laboratory animals,[1,2] and has also been reported to have a protective effect with respect to many aspects of cardiac mechanical function via diverse mechanisms.[3–5] Recently, Shinmura et al. noted that short-term CR may be useful in the clinical setting, having found that the ischemic tolerance of hearts was improved after short-term, graded CR (10% food reduction for 2–3 weeks/35% food reduction for 2 weeks) in rats[6] and mice.[7] In these studies, the effects of CR on life span, age-related physiological functions, and cardiac function were investigated under relatively long-term (3 weeks to 8 months or over), mild calorie restriction (30%–40% reduction in calorie intake over ad-libitum fed animals) conditions in senescent rats. Furthermore, the effects of CR on cardiac function appeared to be independent of the period of CR and age of animals.

In contrast to CR, starvation and severe food restriction do not extend the life span since they lead to malnutrition. Although some studies have found that cardiac function was improved under starvation[8,9] or severe food restriction conditions,[9] it has been reported that the functional properties of rat hearts were depressed after 75% food restriction for 6 weeks.[10] Thus, the relationships between cardiac adaptation and severe food restriction (over 70% food restriction) seem to be inconsistent and not necessarily clarified. Therefore, it would be interesting to compare the nature of myocardial ischemic tolerance induced by severe, short-term food restriction with that produced by usual CR and to clarify the mechanism by which severe, short-term food restriction attenuates myocardial ischemia/reperfusion injury.

In this study, we investigated the effects of severe (70% reduction in food intake on that of ad-libitum fed rats), short-term (11 days) food restriction on cardiac functions, high-energy phosphate metabolite contents, and lactate release into coronary effluent during ischemia/reperfusion with Langendorff perfusion in the isolated hearts of young (10-week-old) male Wistar rats. We also estimated the systemic nutritional state and measured tissue glycolytic metabolite contents, glycolytic enzyme activities, adenosine triphosphatase (ATPase) activities, as well as expressions of functional proteins related to glycolysis, fatty acid utilization, and Ca-handling. We found that the improved ischemic tolerance of the hearts due to severe, short-term food restriction had different characteristics from that induced by usual CR.

Materials and methods

All experiments were performed in accordance with the National Defense Medical College Institutional Animal Care and Use Committee Guidelines.

Treatment of animals

Seven-week-old male Wistar rats were maintained under specific pathogen-free conditions on a constant dark/light cycle (12 h each) in our animal facility throughout the study, and given free access to CE-7 laboratory chow (Clea Japan, Tokyo, Japan) and water for a week before the experiments. Since the mean daily food consumption in this period was 33 g/rat, the daily quantity of food for the rats in the food-restricted group was set at 10 g/rat. A total of 35 rats were used in the present study: 11 for cardiac function measurement and ^{31}P-nuclear magnetic resonance (^{31}P-NMR) spectroscopy (ad-libitum fed group [AL; $n = 5$]; food-restricted group [FR; $n = 6$]), and 24 for the measurement of blood serum and cardiac tissue components (AL, $n = 11$ and FR, $n = 13$). On the first day of the two experiments, the rats were weighed and randomly assigned to either the AL group or FR group and the mean body weights of the two groups were made nearly equal. The FR rats were individually housed and received a daily quantity of food equal to 10 ± 1 g (approximately 70% reduction on food intake of AL group) from 09:00 h to 10:00 h for 11 days. The CE-7 laboratory chow contained 63.8% carbohydrate, 17.6% protein, 3.7% fat, and 341 kcal per 100 g of weight. Based on the National Academy of Science's daily minimal requirements for growing male Sprague-Dawley rats, the 10-g ration of CE-7 chow provided the FR rats with approximately 60% of their gross energy requirements, 98% and 49% of their respective protein and fat requirements, and sufficient levels of vitamins and minerals except for vitamin B_{12} and copper whose levels were 48% and 80% of requirements, respectively.[11] The AL rats received food ad libitum. All rats in the two groups had free access to water and were weighed every 24 h at 10:00 h.

Measurement of cardiac function and ^{31}P-NMR spectroscopy

Heart preparation and perfusion method

Measurements were performed for rats in both groups from 1 to 4 h after the last day's feeding for the FR group. Each rat was premedicated with heparin (1000 U, intraperitoneally [i.p.]) and anesthetized with ketamine (90 mg/kg, i.p.) and xylazine (10 mg/kg, i.p.). The hearts were excised, put into ice-cold modified Krebs–Henseleit buffer, quickly trimmed, weighed, and perfused in the Langendorff mode at a constant perfusion pressure of 100 cmH_2O at 37°C with modified Krebs–Henseleit buffer solution consisting of NaCl 116 mM, KCl 4.7 mM, $MgSO_4$ 1.2 mM, $CaCl_2$ 2.5 mM, $NaHCO_3$ 25 mM, and glucose 11 mM. The buffer solution was continuously aerated with 95% O_2 + 5% CO_2, and the pH was adjusted to 7.4. Heart function was monitored and recorded continuously throughout the experiments using a fluid-filled left ventricular balloon in line with a transducer (P-50, Gould, Valley View, OH, USA) and a WS-641G multichannel recorder (Nihon Kohden, Tokyo, Japan). The balloon volume was set to produce a left ventricular end-diastolic pressure (LVEDP) of 5 mmHg. Each heart was perfused for 15–20 min (control perfusion) and then subjected to 20 min of global ischemia by clamping the aortic cannula, followed by 30 min of reperfusion. The coronary effluent was collected at 5-min intervals throughout the experiments. After the volume of the effluent was measured, some of it was frozen and stored at –80°C until analysis of lactate content, and creatine kinase (CK) and lactic dehydrogenase (LDH) activities.

NMR spectroscopy

All ^{31}P-NMR spectra were obtained using a Bruker AM-360 WB spectrometer, operating at 161.9 MHz with a pulse width of 45°, 120 transients, and a recycle time of 1 s, using a Bruker 20-mm broadband probe maintained at 37°C. Three control ^{31}P-NMR spectra were obtained at 3-min intervals during the control perfusion before ischemia. Spectra were then obtained at 0, 5, 10, and 15 min during ischemia, and at 0, 5, 10, 15, 20, and 25 min during reperfusion. Inorganic phosphate, adenosine triphosphate (ATP), and phosphocreatine (PCr) values for the ischemia and reperfusion periods were quantified through comparison with spectra obtained for a standard solution (KH_2PO_4, 40 μM solution) in a heart-sized glass sphere before the experiments. The intracellular pH (pHi) was calculated from the distance of the chemical shifts between the inorganic phosphorus (P_i) and PCr peaks using the equation $pH = 6.9 - \log(\delta - 5.805)/(3.29 - \delta)$.[12] The free induction decay was multiplied by an exponential function corresponding to 20-Hz line broadening preceding Fourier transformation using the Nuts software (Acorn NMR, Livermore, CA, USA).

Measurement of blood serum and cardiac tissue components

Blood and heart tissue sampling

Measurements were performed for rats in both groups according to the same time schedule as described above. After anesthetizing the rats, the abdomen was opened, blood was collected from the abdominal aorta, and then heparin was injected before removing the heart. After removal, hearts were perfused for 2–5 min in the same manner as for cardiac function measurements. This was done to wash out any remaining blood in the heart tissue and bring the condition of hearts into line with that just after the beginning of the perfusion of isolated hearts for the cardiac function measurements. Then, the hearts were freeze-clamped with aluminum tongs precooled in liquid nitrogen, powdered with a mortar and pestle in liquid nitrogen, and stored at –80°C until measurement of tissue components. The supernatant serum of the collected blood was also stored at –80°C until chemical analysis. Some of the serum was deproteinized by treating with perchloric acid and the resulting supernatant was stored at –80°C for the measurement of lactate and pyruvate concentrations.

Subcellular fractionation

Powdered cardiac tissues were homogenized in 10 parts by weight of ice-cold buffer containing 25 mM Hepes, 250 mM sucrose, 4 mM ethylenediamine tetra-acetic acid (EDTA, 25 mM benzamidine, and 0.2 mM phenylmethylsulfonyl fluoride at pH 7.4 supplemented with proteinase inhibitor cocktail (Complete Mini; Roche, Basel, Switzerland).[13] Homogenates were centrifuged at 600×*g* for 10 min at 4°C (supernatant 1 and crude nuclear fraction). The crude nuclear fraction was resuspended in homogenization buffer, layered on an ice-cold buffer containing 0.9 M sucrose, 50 mM Tris–HCl, 1 mM EDTA, and 25 mM KCl at pH 7.5,[14] and then centrifuged at 1800×*g* for 20 min at 4°C. The pelleted nuclei were resuspended in 40% glycerol, 50 mM Tris–HCl, 5 mM $MgCl_2$, and 0.1 mM EDTA at pH 8,[14] and stored at –80°C. Supernatant 1 was then centrifuged at 10,000×*g* for 10 min at 4°C (supernatant 2 and crude mitochondrial fraction). The crude mitochondrial fraction was resuspended in a buffer containing 210 mM mannitol, 70 mM sucrose, 1 mM EDTA, and 10 mM Hepes at pH 7.5, and 1% Triton X-100,[15] and stored at –80°C. Supernatant 2 was centrifuged at 150,000×*g* for 2 h at 4°C. The resulting supernatant was stored at –80°C as a cytosol fraction. The final membrane pellet was resuspended in homogenization buffer by passing repeatedly through a 29-gauge needle, and stored at –80°C as a microsome fraction. The protein concentration in all fractions was determined by the BCA protein assay method.

Western blot analysis of proteins in each subcellular fraction

Five to thirty micrograms of proteins extracted from each subcellular fraction were separated using sodium dodecyl sulfate–polyacrylamide gel electrophoresis and blotted on a polyvinylidene fluoride membrane (Amersham, Bucks, UK). Blots were blocked for 1 h at room temperature with 5% nonfat dry milk in phosphate-buffered saline supplemented with 0.1% Tween-20 (PBS-T). Primary antibodies against myocyte enhancer factor 2A (MEF2A; 1:1000, Santa Cruz Biochemical, Santa Cruz, CA, USA), peroxisome proliferator activated receptor α (PPARα; 1:1000, Santa Cruz), glucose transporter 1 (GLUT1; 1:300, Santa Cruz), glucose transporter 4 (GLUT4; 1:1000, Santa Cruz), sarcoplasmic reticulum Ca-ATPase (SERCA2; 1:1000, Santa Cruz), phospholamban (PLB; 1:1000, Upstate Biochemical, Lake Placid, NY, USA), Na^+,K^+-ATPase (1:1000, RBI, Natick, MA, USA), Na–H exchanger (NHE; 1:1000, Chemicon International, Temecula, CA, USA), and mitochondrial voltage-dependent anion channel 1 (VDAC1; 1:1000, Santa Cruz) were used. Glyceraldehyde-3-phosphate dehydrogenase (1:1000, Santa Cruz) and actin (1:1000, Santa Cruz) were used as internal controls for the cytosol fraction and other fractions (microsome and mitochondrial fractions), respectively. Each blot was incubated with the corresponding primary antibodies overnight in 1% nonfat dry milk in PBS-T and washed twice in PBS-T. Then the blots were incubated for 1 h with secondary antibodies (Santa Cruz) at the manufacturer's recommended dilution in 1% nonfat dry milk in PBS-T. Immunodetection was performed by means of ECL plus (Amersham Bioscience), and signals were quantified using a LAS 3000 image analyzer (Fuji Film, Tokyo, Japan). Each protein signal intensity in the FR group was normalized with the mean value of that in the AL group.

Enzyme activity assay for each subcellular fraction

ATPase activities were measured according to the methods of Nørby (Na^+,K^+-ATPase),[16] Chu et al. (Ca^{2+}-ATPase),[17] and McEnery and Pedersen (F1-ATPase).[18] Glycolytic enzyme activities were measured according to the methods of Easterby and Quadri (hexokinase, HK),[19] Storey (phosphofructokinase, PFK),[20] Cardenas (pyruvate kinase, PK)[21] and Lee and Goldberg (lactate dehydrogenase, LDH).[22] All enzyme activities were expressed as amounts of decrease or increase in NADH or NADPH/min per μg protein extracted.

Chemical analyses

Cardiac tissue glucose and glycogen contents were fluorometrically determined by the method of Keppler and Decker.[23] Serum cholesterol, triglyceride, high-density lipoprotein cholesterol (HDL-C), free fatty acid (FFA), and glucose levels were determined using an enzyme assay kit (Kyowa Medical, Tokyo, Japan). Serum thyroid-stimulating hormone (TSH), free tri-iodothyronine (fT3), and free thyroxine (fT4) levels were determined using a chemiluminescent immunoassay kit (Bayer Healthcare, Leverkusen, Germany). Serum insulin was measured using a rat insulin radioimmunoassay kit (Linco Research, St. Charles, MO, USA). The other serum components were measured using

a Hitachi 7600 autoanalyzer. Lactate and pyruvate in the deproteinized serum and lactate in the coronary effluent were analyzed enzymatically by the method of Lowry and Passonneau.[24]

Statistical analysis

All values are expressed as mean ± SE. Cardiac function and NMR data were analyzed by means of time-series analysis of variance, and then the differences between the mean values in the AL group and FR group at each measurement time were analyzed using the unpaired Student *t*-test. For the other data, differences between the mean values in the two groups were also analyzed using the unpaired Student *t*-test. Software used for statistical analysis was SAS version 8.1 and Stat View for Windows version J-5.0 (SAS, Cary, NC, USA). $P < 0.05$ was considered as significant.

Results

Cardiac function in Langendorff perfused hearts

During the preischemic perfusion, the coronary flow rate (CFR) in the FR group was significantly higher than in the AL group. Absolute values of maximal positive and negative peaks of the first derivative of left ventricular pressure (+dP/dT and −dP/dT) in the FR group (2422 ± 161 and −1282 ± 51) were significantly lower than in the AL group (2971 ± 156 and −1538 ± 74, respectively), but no significant difference was observed in the other heart function parameters between the AL and FR groups (Table 1).

The LVEDP in the FR group was significantly lower than in the AL group at the end of ischemia. During the 30 min of reperfusion, although CFR, +dP/dT, and −dP/dT did not recover in the AL group, the values of these parameters in the FR group recovered to near the preischemic values. After reperfusion, recoveries in the other cardiac function parameters (left ventricular developed pressure [LVDP] and LVEDP) were more remarkable in the FR group than in the AL group.

Energy metabolite contents and intracellular pH

The ATP content in both groups decreased in a similar manner during ischemia but its recovery in the FR group was significantly greater than in the AL group during reperfusion (Fig. 1A). Interestingly, the PCr content in the FR group was significantly higher than in the AL group at the second measurement point during the control perfusion (Fig. 1B). After reperfusion, the PCr content in the FR group had recovered to near the control level, though the recovery in the AL group was limited (only 42% ± 9%, Fig. 1B). The other parameters (P_i content and pHi) recovered to a greater extent in the FR group than in the AL group during reperfusion (Fig. 1C and D).

Lactate, CK, and LDH release into coronary effluent

Lactate release into the coronary effluent over the 5 min of the control perfusion was significantly lower in the FR group than in the AL group (Fig. 2). However, it was inversely higher in the FR group than in the AL group during the first 5 min of reperfusion. Thereafter, it decreased

Table 1. Hemodynamic parameters from pre-ischemia to end of reperfusion in Langendorff perfused hearts

	Preischemia	End of ischemia	Reperfusion, min		
			10	20	30
CFR, ml/min/g dry weight					
AL group	47.1 ± 1.3	0	25.4 ± 1.4	30.3 ± 1.5	31.3 ± 1.4
FR group	63.0 ± 3.1*	0	62.5 ± 4.4*	61.7 ± 2.5*	57.7 ± 3.0*
LVDP, mmHg					
AL group	111.7 ± 3.9	0	21.8 ± 5.6	31.4 ± 8.0	43.0 ± 7.8
FR group	108.4 ± 8.1	0	69.7 ± 17.4*	95.1 ± 19.3*	99.6 ± 18.1*
LVEDP, mmHg					
AL group	4.0 ± 0.4	46.1 ± 2.6	70.9 ± 4.1	63.7 ± 4.2	57.4 ± 4.5
FR group	4.2 ± 0.7	27.7 ± 4.9*	16.6 ± 3.7*	14.0 ± 3.4*	12.2 ± 3.8*
HR, beats/min					
AL group	191 ± 9	0	120 ± 17	171 ± 13	172 ± 8
FR group	174 ± 13	0	226 ± 44	209 ± 50	206 ± 47
+dP/dT					
AL group	2971 ± 156	0	402 ± 106	730 ± 198	1013 ± 214
FR group	2422 ± 161*	0	1567 ± 357*	2081 ± 369*	2250 ± 386*
−dP/dT					
AL group	−1538 ± 74	0	−247 ± 59	−421 ± 105	−562 ± 102
FR group	−1282 ± 51*	0	−884 ± 191*	−1190 ± 183*	−1257 ± 189*

Values are mean ± SE

AL group, ad-libitum fed group; FR group, food restriction group; CFR, coronary flow rate; LVDP, left ventricular developed pressure; LVEDP, left ventricular end-diastolic pressure; HR, heart rate; +dP/dT and −dP/dT, maximal positive and negative peak of first derivative of left ventricular pressure

* $P < 0.05$ vs. data in corresponding AL group

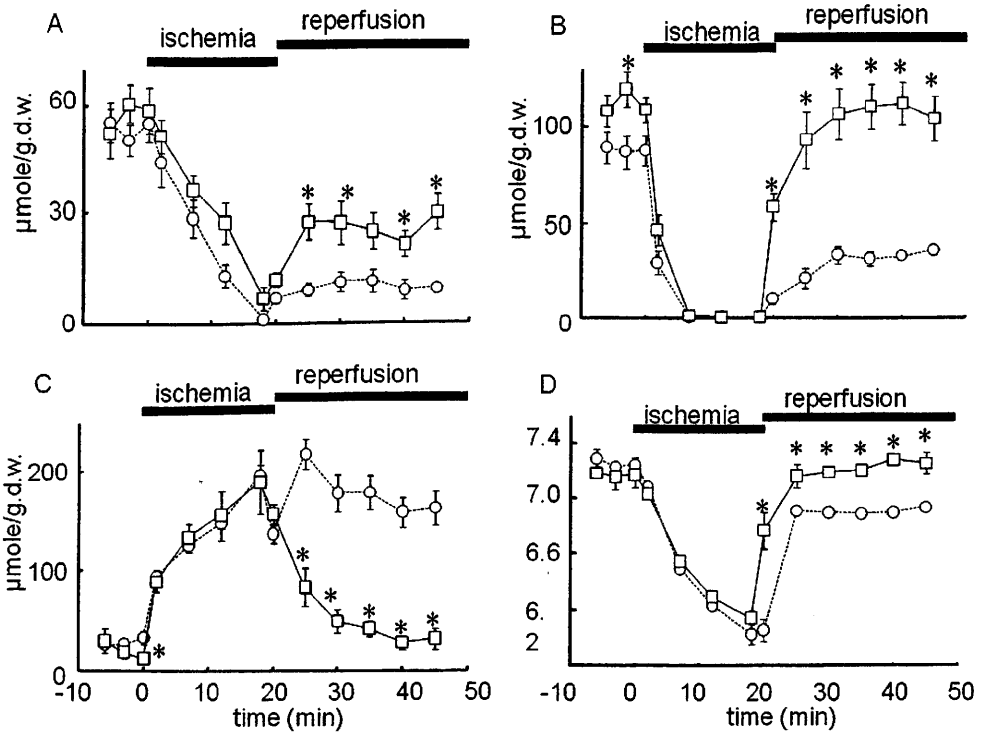

Fig. 1. Changes in adenosine triphosphate (*ATP*) (**A**), phosphocreatine (*PCr*) (**B**), and inorganic phosphorus (P_i) (**C**) contents, and intracellular pH (*pHi*) (**D**) in the hearts of the ad-libitum fed (AL; *circles*) and food restriction (FR; *squares*) groups during ischemia and reperfusion. Data are shown as mean ± SE. *$P < 0.05$ vs the corresponding value in the AL group

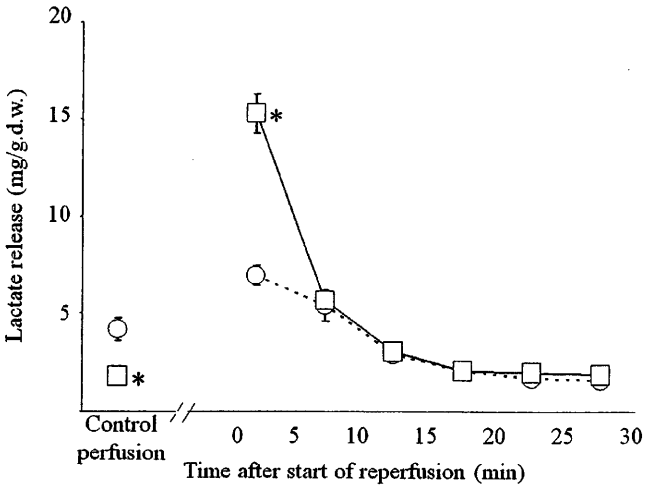

Fig. 2. Release of lactate into the coronary effluent of the hearts in the AL (*circles*) and FR (*squares*) groups during control perfusion and after reperfusion. *$P < 0.05$ vs the value in the AL group

in a similar fashion in the two groups and, after 20 min of reperfusion, had reached a level close to that of the control for the FR group. There was no difference in CK and LDH release during reperfusion between the FR and AL groups (data not shown).

Body weight, heart weight, and food consumption

During the experimental period, the body weight in the AL group increased by 29% (Table 2) while that in the FR group decreased by 21% during the 11 days beginning on the day the amount of feed was restricted to 10 ± 1 g/day.

Table 2. Body weight, heart weight, and average daily food consumption during experimental period

	AL group $n = 16$	FR group $n = 19$
Body weight (g) pre[a]	296 ± 2.2	298 ± 1.7
Body weight (g) post[a]	381 ± 4.3	235 ± 2.3*
Mean food consumption (g/day)	33 ± 1	10 ± 1*
Heart weight (g) wet	1.10 ± 0.03	0.75 ± 0.01*
Heart/body weight ratio (g/kg × 10^3)[b]	2.89 ± 0.05	3.18 ± 0.06

Values are mean ± SE
[a]Pre and post indicate data at the start and end of experiment, respectively
[b]Wet heart weight/body weight post
*$P < 0.05$ vs. data in AL group

The heart weight in the FR group was 68% of that in the AL group ($P < 0.05$). Although the mean heart weight/body weight ratio in the FR group was slightly higher than in the AL group, the difference was not large enough to imply the presence of myocardial hypertrophy or edema.

Serum component levels and heart tissue glucose and glycogen contents

Serum TSH, fT3, fT4, triglyceride, FFA, glucose, and insulin levels were significantly lower in the FR group than in the AL group (Table 3). Serum fT3 and fT4 levels in the FR group decreased by 25% and 19%, respectively, compared with those in the AL group. On the other hand, serum lactate, pyruvate, creatine, Na, and Cl were significantly higher in the FR group than in the AL group. There was no significant difference in serum LDH, CK, total protein, albumin, total cholesterol, and HDL-C concentrations

between the AL group and FR group at the end of the experiments. Serum 3-hydroxybutyrate was significantly higher in the FR than in the AL group, while the acetoacetic acid level was similar in both groups. The tissue glucose content was significantly higher in the FR group than in the AL group.

Table 3. Serum component levels, and cardiac tissue glucose and glycogen contents in AL and FR groups

	AL group $n = 11$	FR group $n = 12$
Serum		
TSH, μIU/ml	2.1 ± 0.3	0.3 ± 0.1*
fT3, pg/ml	3.6 ± 0.1	2.7 ± 0.1*
fT4, ng/dl	2.6 ± 0.1	2.1 ± 0.1*
LDH, IU/l	701 ± 132	668 ± 97
CK, IU/l	540 ± 87	477 ± 46
Total protein, g/dl	5.4 ± 0.1	5.3 ± 0.1
Albumin, g/dl	3.6 ± 0.1	3.6 ± 0.1
Creatinine, mg/dl	0.25 ± 0.01	0.31 ± 0.01*
Na, mEq/l	141 ± 0.5	145 ± 0.5*
K, mEq/l	4.1 ± 0.2	4.3 ± 0.2
Cl, mEq/l	102 ± 0.5	106 ± 0.5*
Lactate, mM	3.12 ± 0.32	5.22 ± 0.86*
Pyruvate, mM	0.22 ± 0.03	0.44 ± 0.07*
Total cholesterol, mg/dl	60 ± 2	60 ± 6
HDL-C, mg/dl	38 ± 1	36 ± 3
Triglyceride, mg/dl	104 ± 8	32 ± 10*
Free fatty acid, mEq/l	0.35 ± 0.03	0.23 ± 0.03*
Acetoacetic acid, μmol/l	88.5 ± 6.9	78.9 ± 8.5
3-Hydroxybutyrate, μmol/l	137.5 ± 8.3	272.5 ± 43.9*
Glucose, mg/dl	292 ± 21	182 ± 22*
Insulin, ng/ml	0.65 ± 0.05	0.21 ± 0.02*
Tissue glucose, μg/mg-tissue wet wt	0.89 ± 0.05	1.12 ± 0.06*
Tissue glycogen, μg/mg-tissue wet wt	3.24 ± 0.31	2.68 ± 0.53

We failed to obtain blood samples for one rat of the FR group, so the number of rats for the analysis of serum components was 12. Values are mean ± SE
TSH, thyroid-stimulating hormone; fT3, free tri-iodothyronine; fT4, free thyroxine; LDH, lactate dehydrogenase; CK, creatine kinase; HDL-C, high-density lipoprotein cholesterol
* $P < 0.05$ vs data in AL group

Glycolytic enzyme and ATPase activities in heart tissues

The amount of protein extracted from each subcellular fraction/g wet weight of heart was nearly the same in the AL and FR groups (data not shown). This result implies that neither the protein content of heart tissue nor that of the subcellular fractions was affected by the 70% food restriction for 11 days. Therefore, despite the difference in mean heart weight between the groups, enzyme activities were expressed as amounts of decrease or increase in NADH or NADPH/min per μg protein extracted. The mean HK activity for the microsome fraction was significantly lower in the FR group (Table 4). There was no significant difference in the activities of other glycolytic enzymes or ATPase activities between the groups for the three subcellular fractions tested.

Western blot analysis of functional proteins

Among the functional proteins examined by Western blot analysis, the expressions of MEF2A in the cytosol fraction, and Na^+,K^+-ATPase and PLB in the microsome fraction were significantly higher in the FR group than in the AL group, but that of VDAC1 in the mitochondrial fraction was significantly lower in the FR group than in the AL group (Fig. 3). There was no difference between the groups in expressions of the other proteins (GLUT1 and GLUT4, SERCA2, and NHE in the microsome fraction, MEF2A in the nuclear fraction, and PPARα in the cytosol fraction).

Discussion

We found that there was a significant recovery in contractile function after reperfusion following global ischemia in the hearts of rats exposed to severe, short-term food restriction. First, among cardiac function parameters we noticed that in the preischemic (control) perfusion, the absolute values of

Table 4. Glycolytic enzyme and ATPase activities in heart tissue subcellular fractions of AL and FR groups

	AL group $n = 11$	FR group $n = 13$
Cytosol fraction		
PK, μg-NADH/min/μg-protein	1.37 ± 0.07	1.38 ± 0.07
PFK, ng-NADH/min/μg-protein	79.8 ± 8.5	78.4 ± 7.1
LDH, μg-NADH/min/μg-protein	5.37 ± 0.11	5.44 ± 0.14
HK, ng-NADPH/min/μg-protein	14.0 ± 0.5	12.3 ± 0.6
Mitochondrial fraction		
HK, ng-NADPH/min/μg-protein	11.2 ± 1.3	8.2 ± 1.2
F_1-ATPase, ng-NADH/min/μg-protein	43.0 ± 3.0	41.6 ± 3.2
Microsomal fraction		
HK, ng-NADPH/min/μg-protein	31.9 ± 2.5	24.6 ± 1.9*
Na^+,K^+-ATPase, ng-NADH/min/μg-protein	127.0 ± 18.3	149.5 ± 24.5
Ca^{2+}-ATPase, ng-NADH/min/μg-protein	109.5 ± 21.8	161.3 ± 22.1

Values are mean ± SE
PK, pyruvate kinase; PFK, phosphofructokinase; LDH, lactate dehydrogenase; HK, hexokinase
* $P < 0.05$ vs. data in AL group

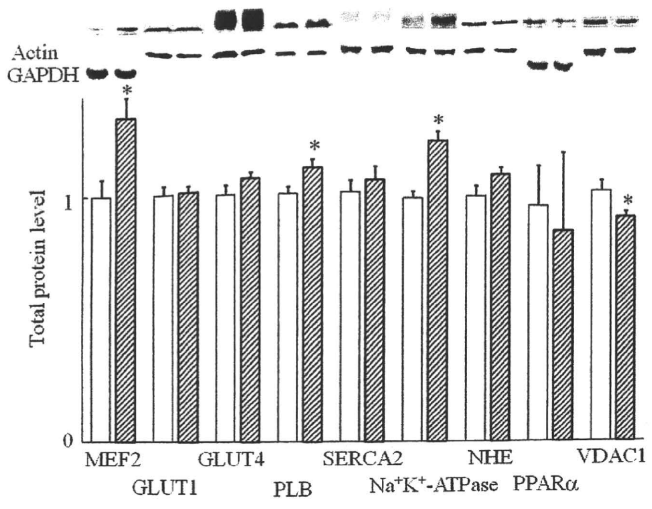

Fig. 3. Western blot analysis of MEF2A and PPARα in the cytosol fraction, GLUT1 and GLUT2, PLB, SERCA2, Na^+,K^+-ATPase, and NHE in the microsome fraction, and VDAC1 in the mitochondrial fraction. *Open bars*, AL group; *hatched bars*, FR group. $*P < 0.05$ vs the value in the AL group. *GAPDH*, glyceraldehyde-3-phosphate dehydrogenase; *MEF2*, myocyte enhancer factor 2A; *GLUT1*, glucose transporter 1; *GLUT4*, glucose transporter 4; *PLB*, phospholamban; *SERCA2*, sarcoplasmic reticulum Ca-ATPase; *NHE*, Na–H exchanger; *PPARα*, peroxisome proliferator activated receptor α; *VDAC1*, mitochondrial voltage-dependent anion channel 1

preischemic +dP/dT and −dP/dt in the FR group were 19% and 17% lower, respectively, than the respective values in the AL group. Blood thyroid hormone levels are generally considered to decrease with food restriction[25] and in line with this, we found that serum fT3 and fT4 levels in the FR group had decreased by 25% and 19% on the AL group levels, respectively. Katzeff et al.[26] reported that the serum T_3 level decreased by 82% and preischemic +dP/dT and −dP/dt by 13% and 18%, respectively, in young female SD rats after 28 days of feeding on a 50% calorie-restricted diet. They also found that the expressions of SERCA2 mRNA and α-myosin heavy chain (MHC) mRNA were suppressed in these animals, and concluded that decreases in the serum T_3 level accompanying chronic calorie-restriction were associated with impaired cardiac contractility due, in part, to alterations in cardiac SERCA2 and MHC gene expression. In our experiments, although there was no suppression of SERCA2 protein expression (Fig. 3), there was a significant increase in PLB expression in the FR group. Thus, our experimental results do not seem to be consistent with those of Katzett et al.[26] The inconsistency may be attributable to differences in the experimental conditions (animals, severity and period of food restriction) used. In our study, we assume that both the decrease in the absolute values of ±dP/dt during the control perfusion and adequate recovery of cardiac function after reperfusion in the FR group were induced by the sustained and increased expressions of SERCA2 and PLB, respectively. Since we could not find any studies showing differences in baseline +dP/dt and −dP/dt between ad-libitum fed and food-restricted animals under mild CR conditions,[3,6] these characteristics (decreased serum T_3 levels and absolute values of ±dP/dt) are assumed to be specific to severe food restriction.

Second, we observed that CFR in the FR group was higher than in the AL group during preischemic perfusion. As a similar finding was reported by Broderick et al.[4] and Klevanov et al.[5] under normal mild CR conditions (they did not measure blood T_3 levels), the increase in CFR is thought to be common to both mild and severe food restriction conditions. The relationship between an increase in CFR and the degree of decrease in serum T_3 levels observed under severe food restriction conditions is still unclear. Although the mechanism underlying this phenomenon should be properly clarified, improved coronary circulation during the control perfusion and reperfusion would enhance the ability to remove toxic metabolic intermediates and modulate cardiac ischemic tolerance.

Third, we noted that the PCr content of the heart tissues was higher and there was less lactate release into the coronary effluent in the FR group than in the AL group during the preischemic period. Since lactate release is a marker of oxidative flux from pyruvate to lactate via lactate dehydrogenase, if we postulate that tissue PCr content is a marker of mitochondrial oxidative activity in cardiac tissue, these results suggest that compared with the AL group, mitochondrial oxidation in the FR group was more highly stimulated in the control perfusion, as suggested by Broderick et al.[27] based on their results obtained under mild food restriction. Although it is not clear whether the higher PCr content in this situation is due to low serum T_3 levels,[28] our results could be related to the systemic metabolic changes described below.

We observed that the protein expressions of Na^+,K^+-ATPase in the microsome fraction and MEF2A in the cytosol fraction were greater in the FR group than in the AL group. Since expression of Na^+,K^+-ATPase in the heart is thought to be positively controlled by thyroid hormone similar to the case of SERCA2,[28] this experimental result may present a contradiction. However, the elevated level of this enzyme in the FR group might more effectively maintain ion transport through sarcolemma in cardiac cells. As MEF2A is thought to regulate the activation of glucose transport via the MEF2A–GLUT4 axis,[29] the greater expression of MEF2A could activate glucose transport, resulting in lower serum glucose levels and higher tissue glucose levels in the FR group as compared with the AL group, though these results are not necessarily consistent with lower insulin levels in the FR group.

We also found that an increase in LVEDP during ischemia was significantly suppressed in the FR group as compared to the AL group, and lactate release into the perfusate during the first 5 min of reperfusion (washout lactate produced during ischemic period) was greater in the FR group than the AL group. These results indicate that oxidation of pyruvate to lactate (anaerobic glycolysis) in the heart tissues was more highly activated during ischemia for the FR group. As shown by Kingsley et al.[30] and Vanoverschelde et al.,[31] activation of glycolytic flux in ischemia is fundamental to effective recovery of cardiac function during reperfusion after ischemia. Thus, the metabolic changes mentioned

above and the greater expression of functional proteins in cardiac tissue that we observed in our study play important roles in the recovery of cardiac functions during reperfusion in the hearts of rats subjected to severe, short-term food-restriction.

Finally, we would like to draw attention to the relationship between systemic metabolic state and cardiac function. The fact that serum triglyceride and FFA levels were lower in the FR group than in the AL group suggests that there was possibly a slight increase in the proportion of glucose with respect to fatty acid in the fuel used by cardiac cells in the FR group.[4] Also, the higher serum lactate and pyruvate levels in the FR group as compared with the AL group suggest that metabolic acidosis was induced systemically. As acidic perfusion is thought to reduce ischemia/reperfusion injury in heart tissue,[32] these metabolic changes might alter metabolism in the cardiac tissue and aid recovery of cardiac function after reperfusion. Furthermore, phosphorylation of adenosine monophosphate-activated protein kinase[6] and increases in serum adiponectin levels[7] have been observed to improve ischemic tolerance under mild food restriction, and the hypoxia inducible factor system[33] and osteopontin[34] are known to play a protective role in ischemia/reperfusion injury. These enzyme and/or cytokine systems may be related to the improved recovery of cardiac function under severe food restriction. In conclusion, our results suggested that cardiac function in isolated, perfused rat hearts was protected against ischemia/reperfusion injury by severe, short-term FR loading via altered expression of functional proteins induced by low serum T_3 levels, decreased coronary conductance, and change in metabolic flux.

Acknowledgments We sincerely thank Toshiaki Musha and Kumiko Ozawa for their excellent technical support.

References

1. Sohal RS, Weindruch R (1996) Oxidative stress, caloric restriction, and aging. Science 273:59–63
2. Weindruch R, Keenan KP, Carney JM, Fernandes G, Feuers RJ, Floyd RA, Halter JB, Ramsey JJ, Richardson A, Roth GS, Spindler SR (2001) Caloric restriction mimetics: metabolic interventions. J Gerontol A Biol Sci Med Sci 56:20–33
3. Abete P, Testa G, Ferrara N, De Santis D, Capaccio P, Viati L, Calabrese C, Cacciatore F, Longobardi G, Condorelli M, Napoli C, Rengo F (2002) Cardioprotective effect of ischemic preconditioning is preserved in food-restricted senescent rats. Am J Physiol Heart Circ Physiol 282:H1978–H1987
4. Broderick TL, Driedzic WR, Gillis M, Jacob J, Belke T (2001) Effects of chronic food restriction and exercise training on the recovery of cardiac function following ischemia. J Gerontol A Biol Sci Med Sci 56:B33–B37
5. Klebanov S, Herlihy JT, Freeman GL (2002) Assessing effects of long-term food restriction on myocardial energetics in the isolated heart preparation. Mech Ageing Dev 123:1375–1388
6. Shinmura K, Tamaki K, Bolli R (2005) Short-term caloric restriction improves ischemic tolerance independent of opening of ATP-sensitive K+ channels in both young and aged hearts. J Mol Cell Cardiol 39:285–296
7. Shinmura K, Tamaki K, Saito K, Nakano Y, Tobe T, Bolli R (2007) Cardioprotective effects of short-term caloric restriction are mediated by adiponectin via activation of AMP-activated protein kinase. Circulation 116:2809–2817
8. Doenst T, Guthrie PH, Chemnitius JM, Zech R, Taegtmeyer H (1996) Fasting, lactate, and insulin improve ischemia tolerance in rat heart: a comparison with ischemic preconditioning. Am J Physiol 270:H1607–H1615
9. Nutter DO, Murray TG, Heymsfield SB, Fuller EO (1979) The effect of chronic protein-calorie undernutrition in the rat on myocardial function and cardiac function. Circ Res 45:144–152
10. Haddad F, Bodell PW, McCue SA, Herrick RE, Baldwin KM (1993) Food restriction-induced transformations in cardiac functional and biochemical properties in rats. J Appl Physiol 74: 606–612
11. Rogers AE, Benevenga NJ, Forbes RM, Nordstrom JW, Wolf G (1978) Nutrient requirements of laboratory animals, 3rd edn. National Academy of Sciences, Washington DC
12. Jacobus WE, Pores IH, Lucas SK, Kallman CH, Weisfeldt ML, Flaherty JT (1981) The role of intracellular pH in the control of normal and ischemic myocardial contractility: a ^{31}P nuclear magnetic resonance and mass spectrometry study. Kroc Found Ser 15:537–65
13. Camps M, Castello A, Munoz P, Monfar M, Testar X, Palacin M, Zorzano A (1992) Effect of diabetes and fasting on GLUT-4 (muscle/fat) glucose-transporter expression in insulin-sensitive tissues. Heterogeneous response in heart, red and white muscle. Biochem J 282:765–772
14. Escher P, Braissant O, Basu-Modak S, Michalik L, Wahli W, Desvergne B (2001) Rat PPARs: quantitative analysis in adult rat tissues and regulation in fasting and refeeding. Endocrinology 142:4195–4202
15. Desagher S, Osen-Sand A, Nichols A, Eskes R, Montessuit S, Lauper S, Maundrell K, Antonsson B, Martinou JC (1999) Bid-induced conformational change of Bax is responsible for mitochondrial cytochrome c release during apoptosis. J Cell Biol 144:891–901
16. Norby JG (1988) Coupled assay of Na^+,K^+-ATPase activity. Methods Enzymol 156:116–119
17. Chu A, Dixon MC, Saito A, Seiler S, Fleischer S (1988) Isolation of sarcoplasmic reticulum fractions referable to longitudinal tubules and junctional terminal cisternae from rabbit skeletal muscle. Methods Enzymol 157:36–46
18. McEnery MW, Pedersen PL (1986) Purification of the proton-translocating ATPase from rat liver mitochondria using the detergent 3-[(3-cholamidopropyl)dimethylammonio]-1-propane sulfonate. Methods Enzymol 126:470–477
19. Easterby JS, Qadri SS (1982) Hexokinase type II from rat skeletal muscle. Methods Enzymol 90:11–15
20. Storey KB (1982) Phosphofructokinase from oyster adductor muscle. Methods Enzymol 90:39–44
21. Cardenas JM (1982) Pyruvate kinase from bovine muscle and liver. Methods Enzymol 90:140–149
22. Lee CY, Yuan JH, Goldberg E (1982) Lactate dehydrogenase isozymes from mouse. Methods Enzymol 89:351–358
23. Keppler D, Decker K (1984) VI: Metabolites 1 carbohydrate. In: Bergmeyer HU (ed) Methods of enzymatic analysis. Academic Press, New York, pp 11–18
24. Lowry O, Passonneau J (1972) A flexible system of enzymatic analysis. Academic Press, New York
25. Merry BJ, Holehan AM (1985) The endocrine response to dietary restriction in the rat. Basic Life Sci 35:117–141
26. Katzeff HL, Powell SR, Ojamaa K (1997) Alterations in cardiac contractility and gene expression during low-T3 syndrome: prevention with T3. Am J Physiol 273:E951–E956
27. Broderick TL, Belke T, Driedzic WR (2002) Effects of chronic caloric restriction on mitochondrial respiration in the ischemic reperfused rat heart. Mol Cell Biochem 233:119–125
28. Klein I, Danzi S (2007) Thyroid disease and the heart. Circulation 116:1725–1735
29. Knight JB, Eyster CA, Griesel BA, Olson AL (2003) Regulation of the human GLUT4 gene promoter: interaction between a transcriptional activator and myocyte enhancer factor 2A. Proc Natl Acad Sci USA 100:14725–14730
30. Kingsley PB, Sako EY, Yang MQ, Zimmer SD, Ugurbil K, Foker JE, From AH (1991) Ischemic contracture begins when anaerobic glycolysis stops: a ^{31}P-NMR study of isolated rat hearts. Am J Physiol 261:H469–H478

31. Vanoverschelde JL, Janier MF, Bakke JE, Marshall DR, Bergmann SR (1994) Rate of glycolysis during ischemia determines extent of ischemic injury and functional recovery after reperfusion. Am J Physiol 267:H1785–H1794
32. Inserte J, Barba I, Hernando V, Abellan A, Ruiz-Meana M, Rodriguez-Sinovas A, Garcia-Dorado D (2008) Effect of acidic reperfusion on prolongation of intracellular acidosis and myocardial salvage. Cardiovasc Res 77:782–790
33. Bai CG, Liu XH, Liu WQ, Ma DL (2008) Regional expression of the hypoxia-inducible factor (HIF) system and association with cardiomyocyte cell cycle re-entry after myocardial infarction in rats. Heart Vessels 23:193–200
34. Wang Y, Chen B, Shen D, Xue S (2009) Osteopontin protects against cardiac ischemia-reperfusion injury through late preconditioning. Heart Vessels 24:116–123

Original

Transient increase in contraction observed during early global ischemia in Langendorff perfused rat heart is glycolysis dependent

Eiichi TAKAYAMA*, Motoaki BESSHO**, Kenya NISHIZAWA***, Tadashi YAMAGISHI***, Shigeki YANAGIDA****, Masatoshi KUSUHARA*****, Fumitaka OHSUZU** and Haruo NAKAMURA******

J. Natl. Def. Med. Coll. (2010) **35** (4) : 184－194

Abstract: A transient increase in contraction (TIC) occurred 20 to 40 sec after the start of global ischemia in the Langendorff perfused rat heart. The TIC did not appear when the heart was perfused with Krebs-Henseleit buffer containing 11 mM 2-deoxyglucose or 5 mM 2-deoxyglucose + 6 mM pyruvate for 3 or 10 min before ischemia initiation. The TIC did not appear when the heart was perfused with buffer containing 150 μM iodoacetate, but was partly evident when it was perfused with 2 mM NaCN containing buffer. When the heart was perfused with buffer containing 30 μM ouabain, there was an obvious inotropy prior to the TIC in ischemia. 10 μM of KB-R7943 had no effect on the occurrence of TIC. The NAD/NADH ratio, an aerobic marker, rapidly decreased, registering about one-fourth of the baseline level after 40 sec of ischemia. There was hardly any change in lactate content, an anaerobic marker, up to 40 sec of ischemia but it suddenly increased after 90 sec of ischemia. ^{31}P-NMR spectroscopy analysis revealed a rapid decrease in creatine phosphate and a concomitant increase in Pi up to 40 sec of ischemia, but showed that the total ATP content hardly changed up to 90 sec of ischemia. During the first 40 sec of ischemia, there was a slight drop in intracellular pH. These results suggest that the TIC observed in early global ischemia of the Langendorff perfused rat heart, occurs during a short period preceding metabolic switching from oxidative phosphorylation to anaerobic glycolysis, and that it is closely connected with glycolysis.

Key words: NAD/NADH ratio ／ Lactate ／ Na^+, K^+-ATPase ／ Energy metabolism ／ Metabolic switching

Introduction

When global ischemia is initiated in the Langendorff-perfused heart, heart function rapidly decreases and finally it ceases to beat in response to its oxygen and metabolic substrate being completely cut off. However, on careful observation, a transient increase in contraction (TIC) can be noticed before the heart stops beating completely.

In the normal beating heart, energy (ATP) is supplied by the cooperative system of oxidative phosphorylation and aerobic glycolysis. Cardiac energy metabolism switches from this aerobic cooperative system to anaerobic glycolysis

* Kasukabe Kisen Hospital, Kasukabe, Saitama 344-0067, Japan
** Department of Internal Medicine, National Defense Medical College, Tokorozawa, Saitama 359-8513, Japan
*** Kawasaki Municipal Kawasaki Hospital, Kawasaki, Kanagawa 210-0013, Japan
**** Maritaime Staff Office, Ministry of Defense, Shinjuku-ku, Tokyo 162-8801, Japan
***** Region Resources Division, Shizuoka Cancer Center Research Institute, Sunto-gun, Shizuoka 411-8777, Japan
****** Mitsukoshi Health and Welfare Foundation, Shinjuku-ku, Tokyo 160-0023, Japan

Received May 27, 2010
Accepted September 9, 2010

when supplies of oxygen (O_2) and/or substrates to heart tissue are cut off by anoxia and/or ischemia[1, 17]. Using surface fluorophotography, it has been detected qualitatively that an increase in intracellular NADH content, a typical ischemic marker, occurs one second after the onset of ischemia[23]. Further, through chemical analysis, intracellular lactate, a marker of anaerobic glycolysis, has been shown to increase more slowly (within the first minute of ischemia or hypoxia)[12, 24]. However, up till now, there have been no studies on the relationship between the increase in lactate content and NADH content or NAD/NADH ratio changes during the early stage of ischemia in Langendorff-perfused rat hearts. Also, it remains to be clarified whether the myocardial dysfunction seen in early ischemia is related to energy metabolite loss, especially that of creatine phosphate[2, 4, 11].

The aim of this study was therefore to clarify the nature of the TIC that occurs in early global ischemia in the Langendorff-perfused rat heart. We first preperfused hearts with metabolic, pump, or exchanger inhibitors before ischemia induction to see if there was any effect on the TIC. Then, when global ischemia had been induced, changes in intracellular pH, and NAD, NADH, lactate, and energy metabolite contents with time were measured chemically or by ^{31}P-NMR spectroscopy. Our results showed that the TIC was closely related to glycolysis and occurred during a short period preceding metabolic switching from the aerobic cooperative system to anaerobic glycolysis in global ischemia.

Methods

Animals and perfusion method

All procedures complied with the *National Defense Medical College Institutional Animal Care and Use Committee Guidelines.*

Male Wistar rats (Charles River Japan Inc.) of 8 to 10 weeks old were used. The rats were given an intraperitoneal injection of heparin (800 U/kg body wt) and anesthetized with xylazine hydrochloride (10 mg/kg) and ketamine hydrochloride (90 mg/kg), also given by intraperitoneal injection. Hearts were excised, quickly arrested in ice-cold Krebs-Henseleit buffer, and then their wet weights were measured. The ascending aortas were cannulated, and the hearts were perfused for 15-20 min (control perfusion) by the Langendorff procedure using Krebs-Henseleit buffer (NaCl 118 mM, KCl 4.7 mM, $CaCl_2$ 2.55 mM, $MgSO_4$ 1.18 mM, KH_2PO_4 1.18 mM, $NaHCO_3$ 24.9 mM, and glucose 11.1 mM; pH 7.3) at a hydrostatic pressure of 100 cmH_2O. The perfusate was equilibrated with a gas mixture of 95% O_2 and 5% CO_2 and maintained at 37°C throughout the experiment. Pulmonary arteries were carefully incised to prevent build-up of venous pressure. Global ischemia was induced by stopping the perfusion.

Measurement of left ventricular function

Twenty-two isolated hearts were perfused as described above. An air-free latex balloon was inserted into the left ventricle via the left atrial appendage, and the left ventricular pressure and heart rate were recorded continuously with a pressure-transducer (P-50, Gould Inc.) equipped with an amplifier (PMP-6004, Nihon Kohden) connected to a recorder (WS-641G, Nihon Kohden) for the duration of the experiment. In the control perfusion, the left ventricular end-diastolic pressure (EDP) was set at approximately 5 mmHg by infusing bubble-free saline into the balloon. Hearts were excluded from the experiment if either the systolic pressure was below 70 mmHg or the heart rate was under 150 beats/min. Then, the hearts were divided into nine groups of two to three hearts each whose perfusion details were as follows: 1) control (n=3), 2) 2-deoxyglucose (2-DG) 11 mM (n=3), 3) 2-DG 5 mM + Na pyruvate 6 mM (n=3), 4) iodoacetate (IAA) 150